Computational Vademecums for Lattice Materials using Algebraic PGD

PhD Candidate: Alberto P. Sibileau

Advisors: Prof. F. Auricchio, Prof. P. Díez

Co-Advisors: Dr. S. Morganti, Dr. A. García González

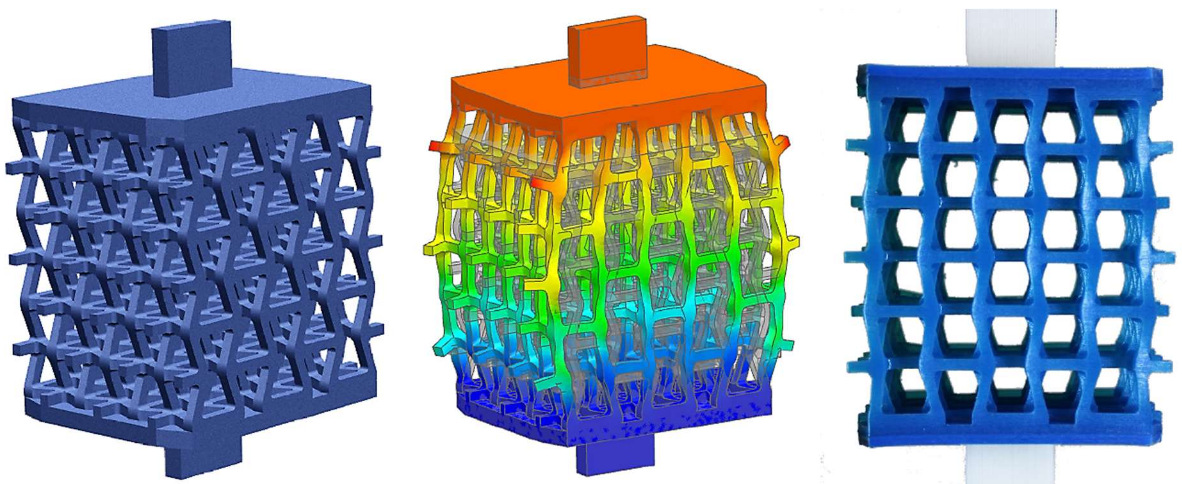

Pavia, September 24th, 2019

Bringing Architecture into Materials

- The evolution of monuments shows us evidence that:

"***The art of structure is where to put the holes***". Robert Le Ricolais (1894 – 1977).

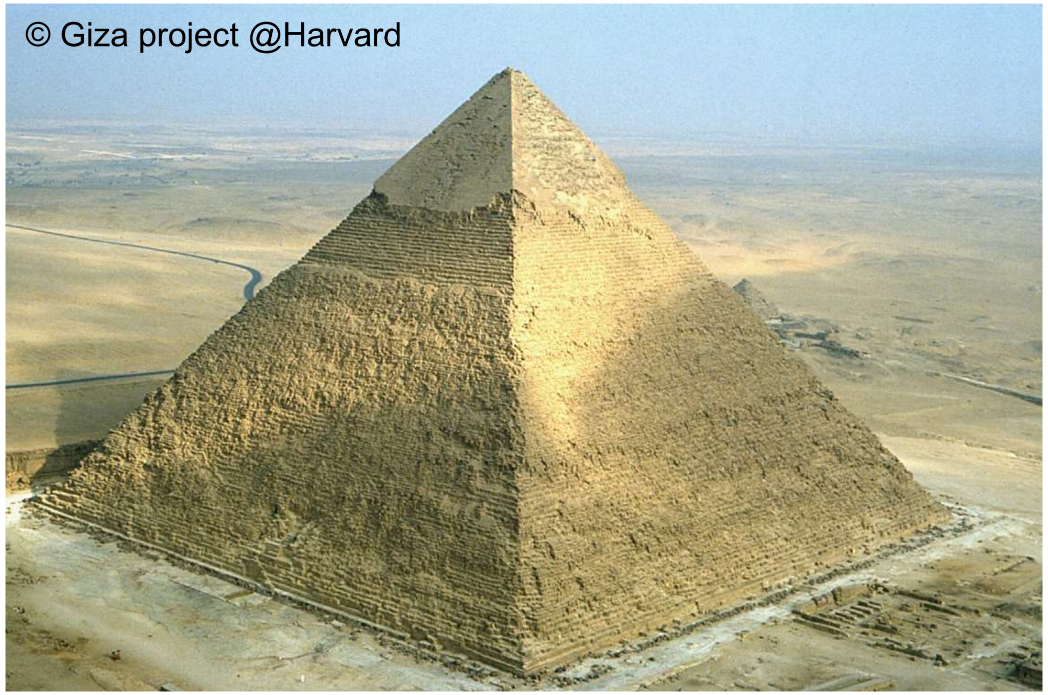

Khafre Pyramid Complex (Giza, 2570 BC)

4459 years

Eiffel Tower (Paris, 1889)

Architected Materials

1. From structure to Architected Materials: it is a matter of scale. For example:

Human femur head cross-section

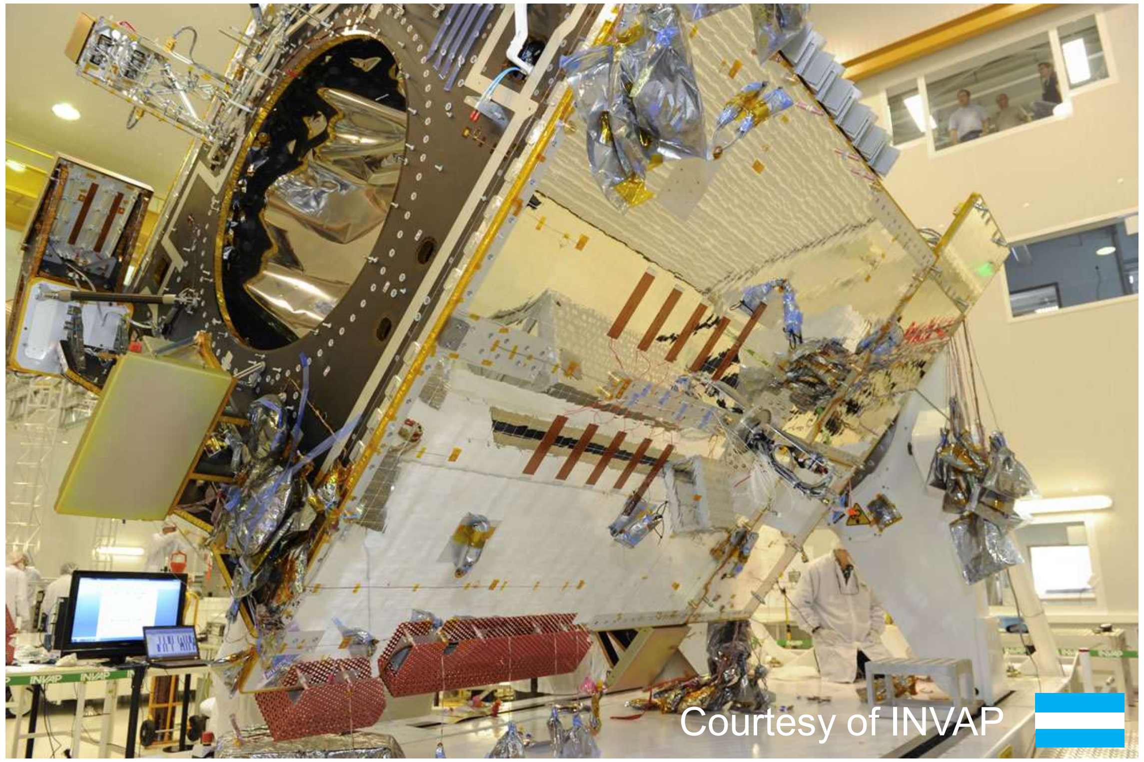

Aerospace engineering uses sandwich panels
(ARSAT I communications satellite)

2. Architected Materials distinguished concept is: we can tailor its properties by designing its internal shape.

Design & Manufacturing: friends or foes?

- Traditionally, research about Architected Materials design and manufacturing has been approach separately.

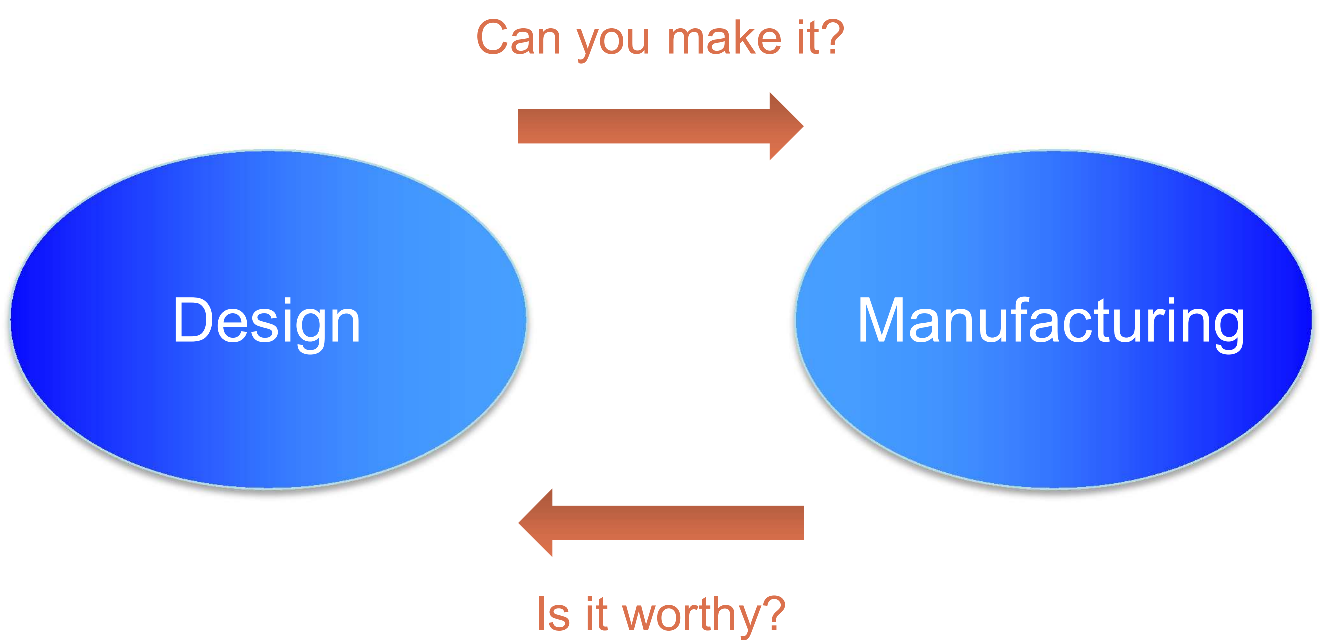

- For example, the first notable contributions answering these questions, have appeared independently:

1994: architected materials design in Computational Mechanics (first paper).

1984: Additive Manufacturing (first patent).

- Today, a positive feedback is promoting Architected Materials: simulation for additive manufacturing.

Lattice Materials

- One type <u>among</u> the family of Architected Materials.
- <u>Structured topology</u>: grid of points connected by <u>slender elements</u>.
- In particular, <u>periodic</u> lattices use the concept of a "<u>unit-cell</u>".

Unit-cell structure:

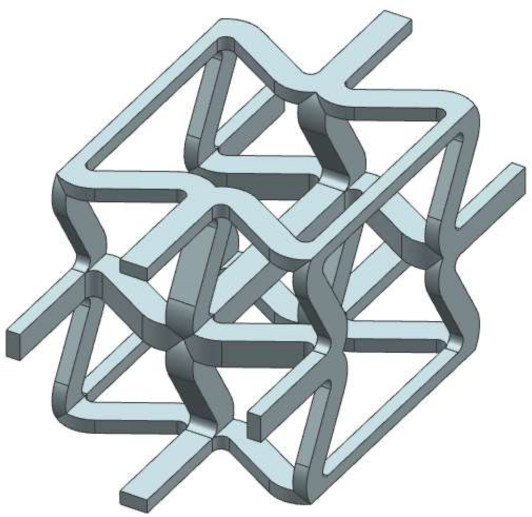

Bulk material:
(5x5x5 tessellation)

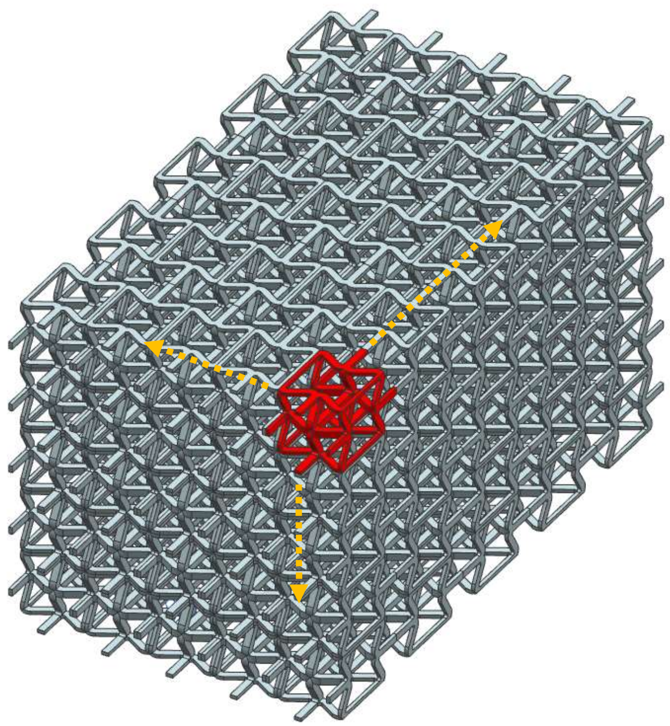

- <u>Application</u>: focus on <u>auxetics</u> (<u>mechanical</u> material property).
- Other <u>fields</u>: wave propagation, electromagnetism, heat conduction, …

Auxetics – Definition & Characteristics

- Materials with negative Poisson's ratio (NPR). This has many characteristics, two of them are:

1. Volume expansion produced by uniaxial stretch:

(auxetic - NPR)

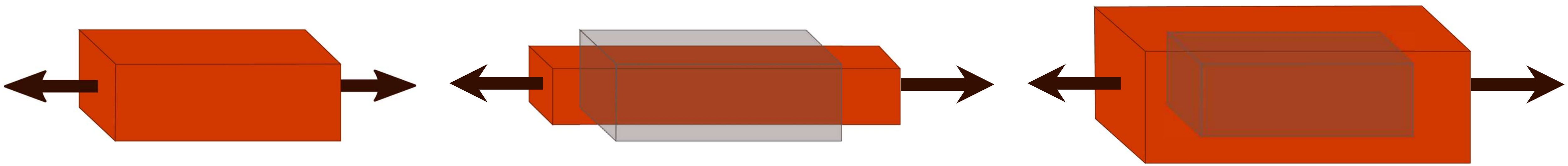

Initial | Deformed: $\nu > 0$ | Deformed: $\nu < 0$

2. Dome shape adopted by a thick plate under bending:

(auxetic - NPR)

Saddle shape: $\nu > 0$ | Dome shape: $\nu < 0$

Auxetics – Applications

1. Tissue engineering scaffolds (Spatial Tuning of Poisson's ratio in scaffolds, *Acta Biomat.*, **2012**):

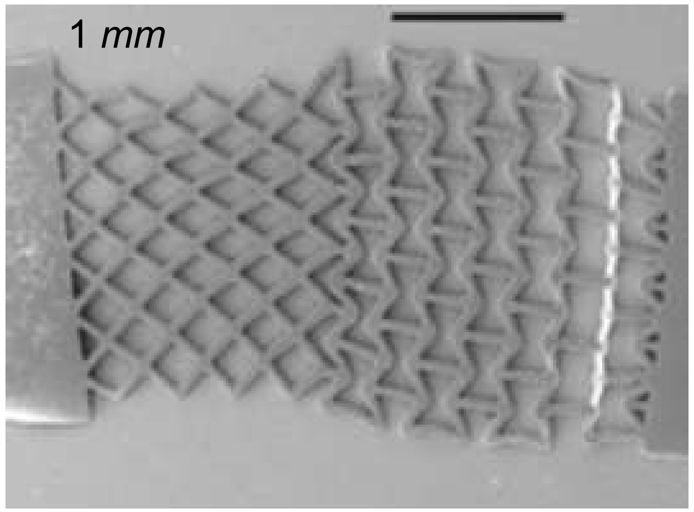

Initial

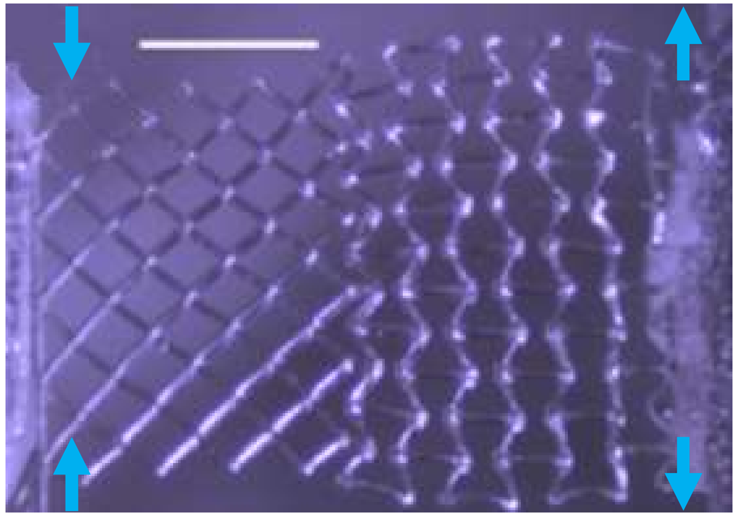

Deformed

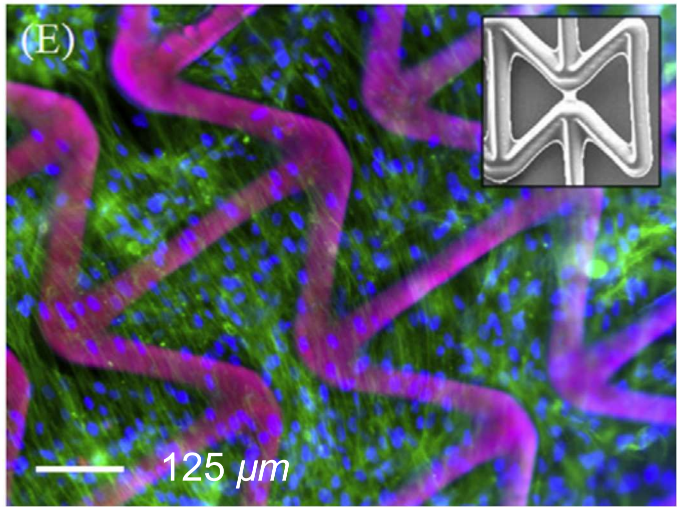

Growing cells

2. Stents (Buckling response of auxetic cellular tubes, *Smart Mater. Struct.*, **2013**):

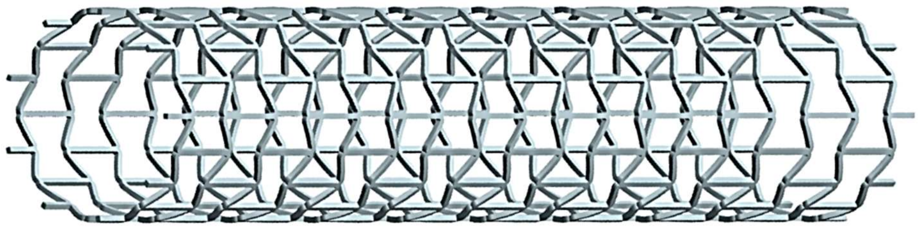

Structure

Kinks induced by bending

Parametric Lattice Materials

- Exploit tailored material properties achieved by parametric design.
- A parametric lattice material is introduced, based on the hexagonal honeycomb (provides auxetic behavior).
- The mechanics is described by Euler-Bernoulli beams, and a unit-cell geometry is introduced.

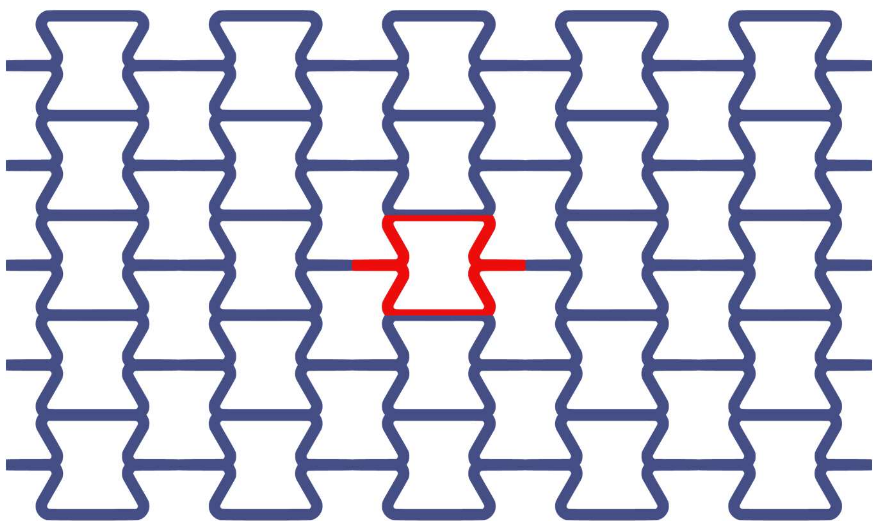

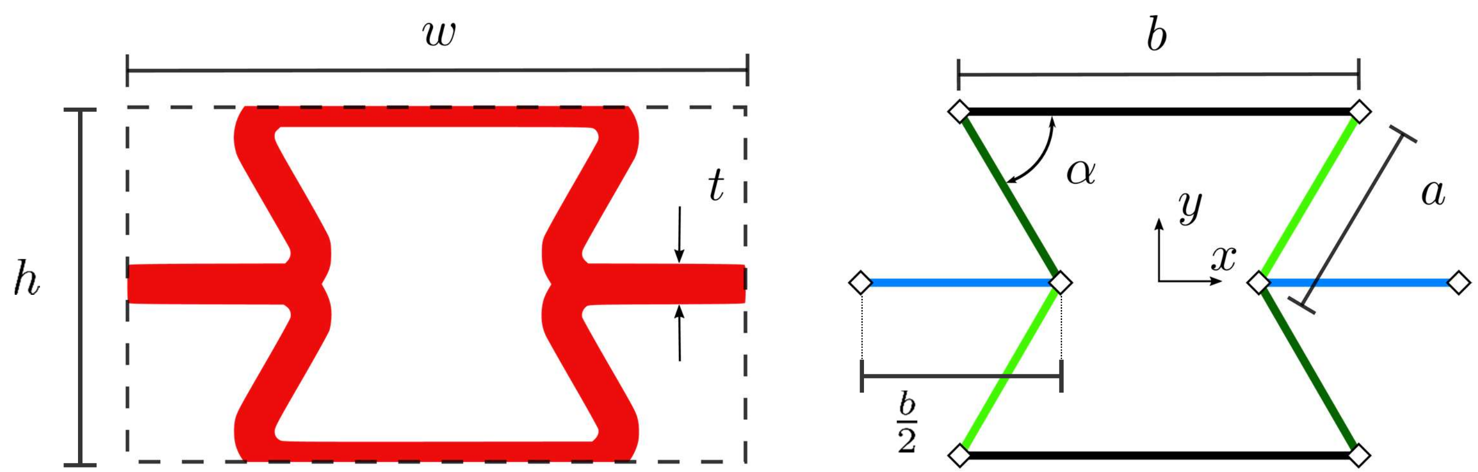

(a) Unit-cell geometry (b) Beams and parameters

- Vector of 4 geometric parameters: $\boldsymbol{\mu} = [a \quad b \quad \alpha \quad t].$
- Geometry imposes constraint on the parameters intervals.

$$\begin{cases} a \in I_1 = [0.3, 0.7]\,, \quad b \in I_2 = [1, 1.5]\,, \\ \alpha \in I_3 = [\frac{\pi}{4}, \frac{3\pi}{4}]\,, \quad t \in I_4 = [\frac{1}{50}, \frac{1}{5}]\,, \end{cases}$$

and animation …

Parametric Solutions by Proper Generalized Decomposition (PGD)

- Solve efficiently and in "one shot" a parametric linear Partial Differential Equation – PDE. (Parametric equilibrium in our lattice material).
- The solutions (known as *Computational Vademecums)* are explicit in the parameters.

↓

Browse the material properties design space as a post-processing (real time).

Contributions

- Use *Computational Vademecums* for optimization or inverse problems. (No need to solve any extra equation + availability of the sensitivities).

↓

Identify design parameters that produce desired material properties.

- Algebraic PGD: a generic solver for parametric PDE's

Discretized parametric PDE – Full Order

- Spatial mesh size: $\mathtt{n_{dof}}$ $\rightarrow$ system of linear equations, depending on $\mathtt{n_p}$ parameters:

$$\mathbf{K}(\boldsymbol{\mu})\,\mathbf{U}(\boldsymbol{\mu}) = \mathbf{F}(\boldsymbol{\mu}), \quad \boldsymbol{\mu} = [\mu_1\ \mu_2\ \ldots\ \mu_{\mathtt{n_p}}], \quad \mathbf{U}(\boldsymbol{\mu}) \in \mathbb{R}^{\mathtt{n_{dof}}}.$$

- Global or multidimensional space $\mathcal{D}$ of the parameters:

$$\mu_i \text{ in } I_i \subset \mathbb{R}\,, \quad \boldsymbol{\mu} \text{ in } \mathcal{D} = I_1 \times I_2 \times \cdots \times I_{\mathtt{n_p}} \subset \mathbb{R}^{\mathtt{n_p}}.$$

- Weighted residuals method:

$$\int_{I_1}\int_{I_2}\cdots\int_{I_{\mathtt{n_p}}} \delta\mathbf{U}(\boldsymbol{\mu})^{\mathsf{T}}\,\mathbf{R}\big(\mathbf{U}(\boldsymbol{\mu})\big)\,\mathrm{d}\mu_{\mathtt{n_p}}\ldots\mathrm{d}\mu_2\,\mathrm{d}\mu_1 = 0,\ \forall\ \delta\mathbf{U}(\boldsymbol{\mu}) \in [\mathcal{L}_2(\mathcal{D})]^{\mathtt{n_{dof}}}\,,$$

$$\text{where } \mathbf{R}(\mathbf{U}(\boldsymbol{\mu})) := \mathbf{F}(\boldsymbol{\mu}) - \mathbf{K}(\boldsymbol{\mu})\,\mathbf{U}(\boldsymbol{\mu}).$$

- Number of unknowns for a numerical solution (Full Order):

$$\mathtt{n_{Full}} = \mathtt{n_{dof}} \prod_{i=1}^{\mathtt{n_p}} \mathtt{n}_{\mathtt{d},i}\,, \quad \mathtt{n}_{\mathtt{d},i}: \text{parameters mesh size.}$$

Separable approximation – Reduced Order

- The unknown is approximated by n terms or "modes" :

$$\mathbf{U}(\boldsymbol{\mu}) \approx \mathbf{U}^n_{\texttt{PGD}}(\boldsymbol{\mu}) = \sum_{m=1}^{n} \mathbf{u}^m \prod_{i=1}^{\mathtt{n_p}} G_i^m(\mu_i)\,, \quad \left\{ \begin{array}{ll} \mathbf{u}^m & : \text{ spatial modes.} \\ G_i^m & : \underline{\text{1D}} \text{ parametric functions.} \end{array} \right.$$

- Number of unknowns for one mode:

$$\left\{ \begin{array}{l} \mathtt{n_{PGD}} = \mathtt{n_{dof}} + \sum_{i=1}^{\mathtt{n_p}} \mathtt{n}_{\mathtt{d},i} << \mathtt{n_{Full}} = \mathtt{n_{dof}} \prod_{i=1}^{\mathtt{n_p}} \mathtt{n}_{\mathtt{d},i}\,. \\ \text{Price to pay: } \underline{\text{nonlinear}} \text{ (product of unknowns).} \end{array} \right.$$

Separable input data requirement

$$\mathbf{K}(\boldsymbol{\mu}) = \sum_{k=1}^{\mathtt{n_k}} \mathbf{K}^k \prod_{i=1}^{\mathtt{n_p}} B_i^k(\mu_i)\,, \quad \mathbf{F}(\boldsymbol{\mu}) = \sum_{\ell=1}^{\mathtt{n_f}} \mathbf{f}^\ell \prod_{i=1}^{\mathtt{n_p}} S_i^\ell(\mu_i)\,.$$

Originality: the Solver box

$$\left.\begin{array}{l}\mathbf{K}(\boldsymbol{\mu}) \longrightarrow \\ \mathbf{F}(\boldsymbol{\mu}) \longrightarrow\end{array}\right. \boxed{\text{Apgd}} \longrightarrow \mathbf{U}(\boldsymbol{\mu})$$

with: $\mathtt{n_{PGD}} << \mathtt{n_{Full}}$

1st : Greedy (sequential computation of terms)

- Start computing $\mathbf{U}^1_{\mathtt{PGD}} \to$ compute $\mathbf{U}^2_{\mathtt{PGD}} \to \ldots \to \mathbf{U}^n_{\mathtt{PGD}}$: $\quad \mathbf{U}^n_{\mathtt{PGD}}(\boldsymbol{\mu}) = \mathbf{U}^{n-1}_{\mathtt{PGD}}(\boldsymbol{\mu}) + \mathbf{u}\prod_{i=1}^{\mathtt{n_p}} G_i(\mu_i).$
- Weighted residuals: find $\mathbf{u}, G_1, G_2, \ldots, G_{\mathtt{n_p}}$ such that:

$$\int_{I_1}\int_{I_2}\ldots\int_{I_{\mathtt{n_p}}} \delta\mathbf{U}(\boldsymbol{\mu})^{\mathsf{T}}\mathbf{R}\big(\mathbf{U}^n_{\mathtt{PGD}}(\boldsymbol{\mu})\big)\,\mathrm{d}\mu_{\mathtt{n_p}}\ldots\mathrm{d}\mu_2\,\mathrm{d}\mu_1 = 0,\ \forall\,\delta\mathbf{U}(\boldsymbol{\mu}), \qquad \delta\mathbf{U} = \underline{\delta\mathbf{u}\prod_{i=1}^{\mathtt{n_p}} G_i} + \underline{\mathbf{u}\sum_{i=1}^{\mathtt{n_p}}\left[\delta G_i \prod_{\substack{j=1\\ j\neq i}}^{\mathtt{n_p}} G_j\right]}$$

2nd : Alternated directions (linearization)

- <u>Fixed-point iterative</u> strategy (leads to a series of local problems):

(Step 1): Compute $\mathbf{u}$ assuming all G_i known for $i = 1, 2, \ldots, \mathtt{n_p}$ $\quad \to \quad \underline{\delta\mathbf{U} = \delta\mathbf{u}\prod_{i=1}^{\mathtt{n_p}} G_i}$

$\text{(Steps } 2\ldots\mathtt{n_p}+1)$: Compute one G_i , assuming $\mathbf{u}$ and all G_j known for $i, j = 1, 2, \ldots, \mathtt{n_p}$ and $j \neq i$

$$\to \quad \underline{\delta\mathbf{U} = \mathbf{u}\,\delta G_i \prod_{\substack{j=1\\ j\neq i}}^{\mathtt{n_p}} G_j}$$

$\mathtt{n_{dof}}$ problem

Build linear system and solve $\mathbf{u}$:

$$\underbrace{\left[\sum_{k=1}^{\mathtt{n_k}} \mathbf{K}^k\, c^k\right]}_{\text{computable matrix}} \mathbf{u} = \underbrace{\sum_{\ell=1}^{\mathtt{n_f}} \mathbf{f}^\ell\, \hat{c}^{\,\ell} - \sum_{m=1}^{n-1}\left[\sum_{k=1}^{\mathtt{n_k}} \mathbf{K}^k\, c^{k,m}\right] \mathbf{u}^m}_{\text{computable vectors}},$$

using

$$\left\{\begin{aligned} c^k &:= \prod_{i=1}^{\mathtt{n_p}} \int_{I_i} \mathrm{B}_i^k\,(\mathrm{G}_i)^2\,\mathrm{d}\mu_i \\ \hat{c}^{\,\ell} &:= \prod_{i=1}^{\mathtt{n_p}} \int_{I_i} \mathrm{S}_i^\ell\,\mathrm{G}_i\,\mathrm{d}\mu_i \\ c^{k,m} &:= \prod_{i=1}^{\mathtt{n_p}} \int_{I_i} \mathrm{B}_i^k\,\mathrm{G}_i^m\,\mathrm{G}_i\,\mathrm{d}\mu_i \end{aligned}\right.$$

1D problems ($\mathtt{n_p}$ times)

Solve G_i :

$$\underbrace{G_i(\cdot)}_{\downarrow} = \frac{\displaystyle\sum_{\ell=1}^{\mathtt{n_f}} \overbrace{(\mathbf{u}^\mathsf{T}\,\mathbf{f}^\ell)}\,\hat{d}_i^\ell(\cdot) - \sum_{m=1}^{n-1}\sum_{k=1}^{\mathtt{n_k}} \overbrace{(\mathbf{u}^\mathsf{T}\,\mathbf{K}^k\,\mathbf{u}^m)}^{\text{computable scalars}}\,d_i^{k,m}(\cdot)}{\displaystyle\sum_{k=1}^{\mathtt{n_k}} \underbrace{(\mathbf{u}^\mathsf{T}\,\mathbf{K}^k\,\mathbf{u})}\,d_i^k(\cdot)},$$

$$\left\{\begin{aligned} d_i^k(\cdot) &= \left(\prod_{j\neq i}\int_{I_j} B_j^k\,(G_j)^2\,\mathrm{d}\mu_j\right) B_i^k(\cdot) \\ \hat{d}_i^\ell(\cdot) &= \left(\prod_{j\neq i}\int_{I_j} S_j^\ell\,G_j\,\mathrm{d}\mu_j\right) S_i^\ell(\cdot) \\ d_i^{k,m}(\cdot) &= \left(\prod_{j\neq i}\int_{I_j} B_j^k\,G_j^m\,G_j\,\mathrm{d}\mu_j\right) B_i^k(\cdot)\,G_i^m(\cdot) \end{aligned}\right.$$

$(\cdot)$: computable function taking values in I_i

<u>Very important use</u> for Greedy & Alternated directions <u>Stopping criteria</u>.

Local Norms

- L_2 norm for the 1D <u>parametric</u> functions: $$\|G_i^m\|^2 = \int_{I_i} (G_i^m)^2 \, \mathrm{d}\mu_i \,, \quad \widetilde{G}_i^m = \frac{G_i^m}{\|G_i^m\|} \,.$$

- <u>Non-Euclidean</u> norm for the <u>spatial modes</u>: $$\|\mathbf{u}^m\|^2 = [\mathbf{u}^m]^{\mathsf{T}} \mathbf{M}_{\mathrm{u}} \, \mathbf{u}^m \,, \quad \widetilde{\mathbf{u}}^m = \frac{\mathbf{u}^m}{\|\mathbf{u}^m\|} \,.$$

- Finally, modal <u>amplitudes</u>: $$\beta^m = \|\mathbf{u}^m\| \prod_{i=1}^{\mathtt{n_p}} \|G_i^m\| \,, \quad \mathbf{U}_{\mathtt{PGD}}^n(\boldsymbol{\mu}) = \sum_{m=1}^{n} \beta^m \, \widetilde{\mathbf{u}}^m \prod_{i=1}^{\mathtt{n_p}} \widetilde{G}_i^m .$$

Motivation

- Greedy computation of terms does not enforce orthogonality between modes.

Objective

- Reduce the PGD solution " n " number of terms while keeping accuracy.

Methodology

- Least-Squares projection of the PGD solution into the same approximation space.

Result

- A new separable approximation computed with the same Greedy + Alternated directions scheme:

$$\mathbf{U}^{\widehat{n}}_{\texttt{com}} = \sum_{\widehat{m}=1}^{\widehat{n}} \widehat{\mathbf{u}}^{\widehat{m}} \prod_{i=1}^{\mathbf{n}_{\mathrm{p}}} \widehat{G}_i^{\widehat{m}} \,, \quad \text{expecting that } \; \widehat{n} < n \,.$$

- Explicit parametric solutions:

2D lattice materials solved by Algebraic PGD

1) Unit-cell with Homogenization

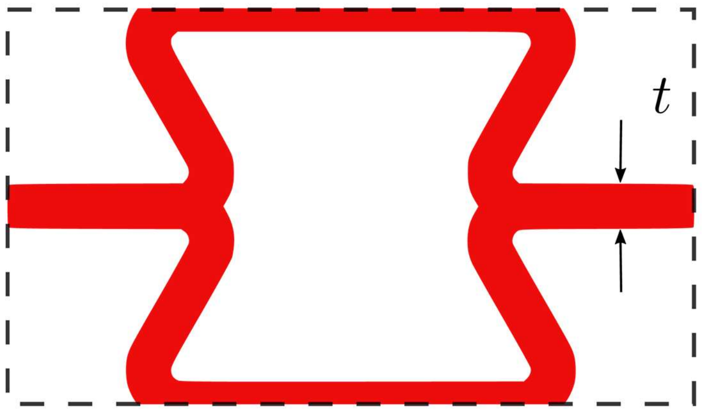

(a) Unit-cell

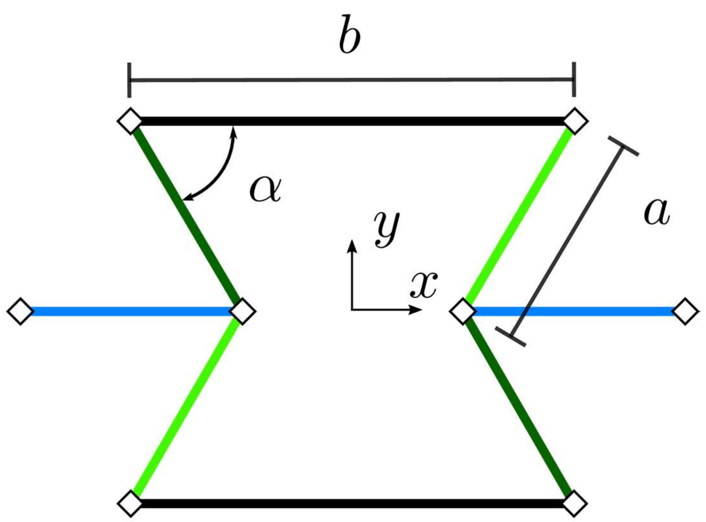

(b) Beams model

Parameters:

$$\boldsymbol{\mu} = [a\ b\ \alpha\ t]$$

a) Separable Input Data.

b) Three load cases: two axial and one shear loads + periodic boundary conditions.

- PGD solver performance.
- Upscaling: recovering the orthotropic material properties at the macro-scale.

Separable Input Data: finite elements + parametric dimensions

- Goal: construct global stiffness Matrix in the separated format (a.k.a. *affine decomposition*)

$$\mathbf{K}(\boldsymbol{\mu}) = \sum_{k=1}^{\mathrm{n_k}} \mathbf{K}^k \prod_{i=1}^{4} B_i^k(\mu_i), \quad \boldsymbol{\mu} = [\mu_1 \ \ \mu_2 \ \ \mu_3 \ \ \mu_4] = [a \ \ b \ \ \alpha \ \ t].$$

FE procedures:

1. Parametric elemental stiffness (for example, elements in Green):

$$\mathbf{K}_e(a, \alpha, t) = \mathbf{T}_e{}^{\mathsf{T}}(\alpha)\, \widehat{\mathbf{K}}_e(a, t)\, \mathbf{T}_e(\alpha)\,.$$

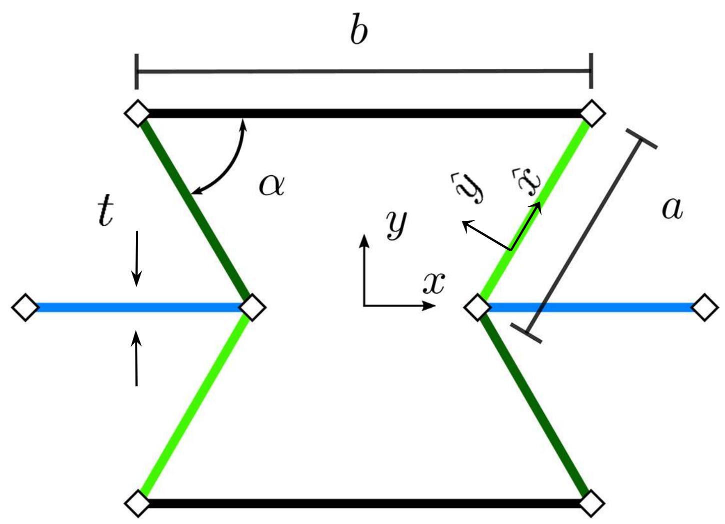

2. Separate $\widehat{\mathbf{K}}_e(a, t)$ and $\mathbf{T}_e(\alpha)$, replace and recover affine decomposition for $\mathbf{K}_e(\boldsymbol{\mu})$. Repeat $\forall e$.

4. Finite element assembly + parametric dependence: affine decomposition for $\mathbf{K}(\boldsymbol{\mu})$

Apgd

PGD Modal Amplitudes

- Three load cases with periodic boundary conditions. Stop Greedy if: $\dfrac{\beta^n}{\max_{m=1,\dots,n}(\beta^m)} < 10^{-4}$.

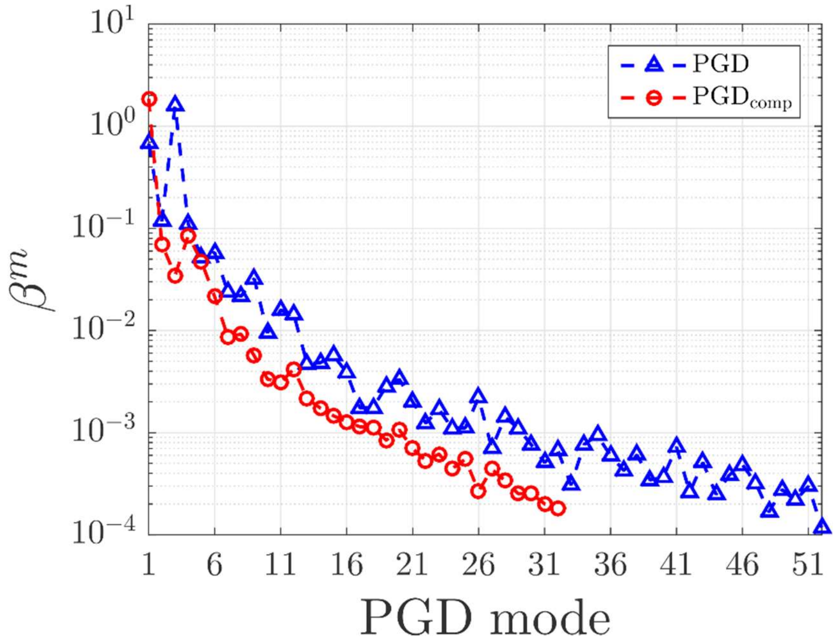

Load XX (52/32)

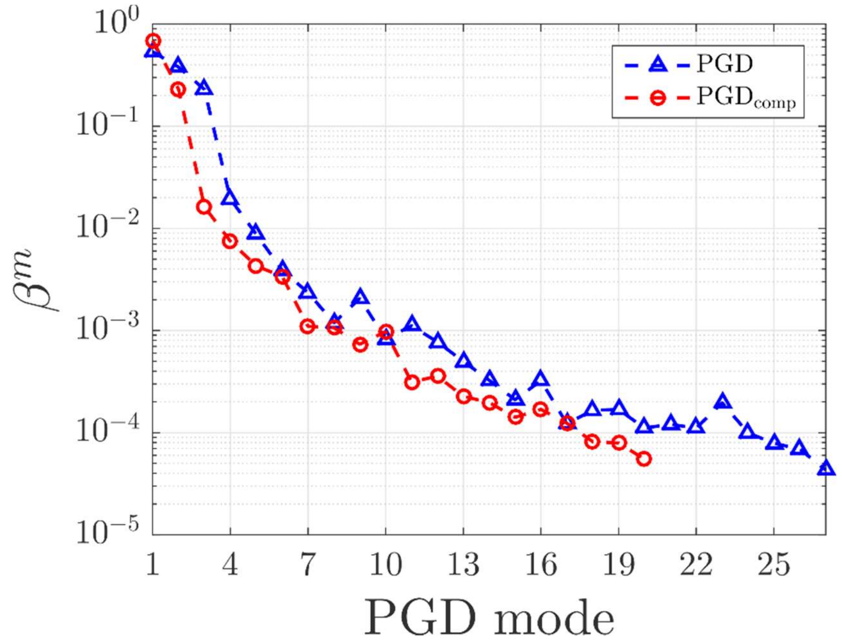

Load YY (27/20)

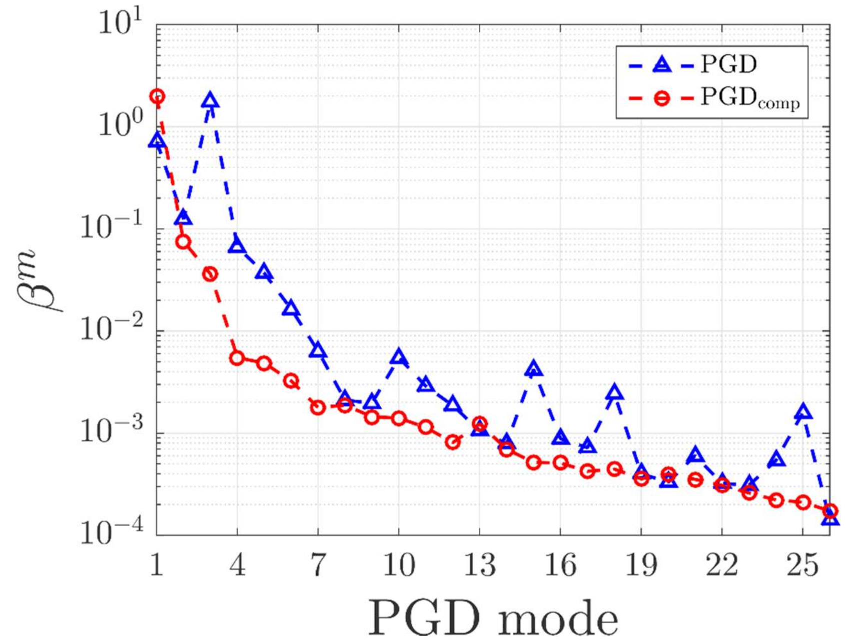

Load XY (26/26)

- Total number of modes comparison between PGD & PGD compression.
- Smoother evolution in PGD compression + terms reduction in load cases *XX* and *YY*.

PGD global performance

- The goal is to show the evolution of the error measured in a global parametric norm.
- We computed symbolically an analytical solution $\mathbf{U}(\boldsymbol{\mu})$. Then, evaluate the relative difference against $\mathbf{U}_{\mathtt{PGD}}(\boldsymbol{\mu})$:

$$\epsilon_{\mathtt{glob}} = \sqrt{\frac{\sum_{\ell=1}\sum_{k=1}\sum_{j=1}\sum_{i=1}\left\|\mathbf{U}(a^i,b^j,\alpha^k,t^\ell)-\mathbf{U}_{\mathtt{PGD}}(a^i,b^j,\alpha^k,t^\ell)\right\|^2}{\sum_{\ell=1}\sum_{k=1}\sum_{j=1}\sum_{i=1}\left\|\mathbf{U}(a^i,b^j,\alpha^k,t^\ell)\right\|^2}},$$

Average of many points distributed in all intervals.

Monotonic error decay.
Error descend rates particularly slow down in *XY*.
Maximum relative error < 0.3% for all loads.
Same stopping criteria $\neq$ same global errors.

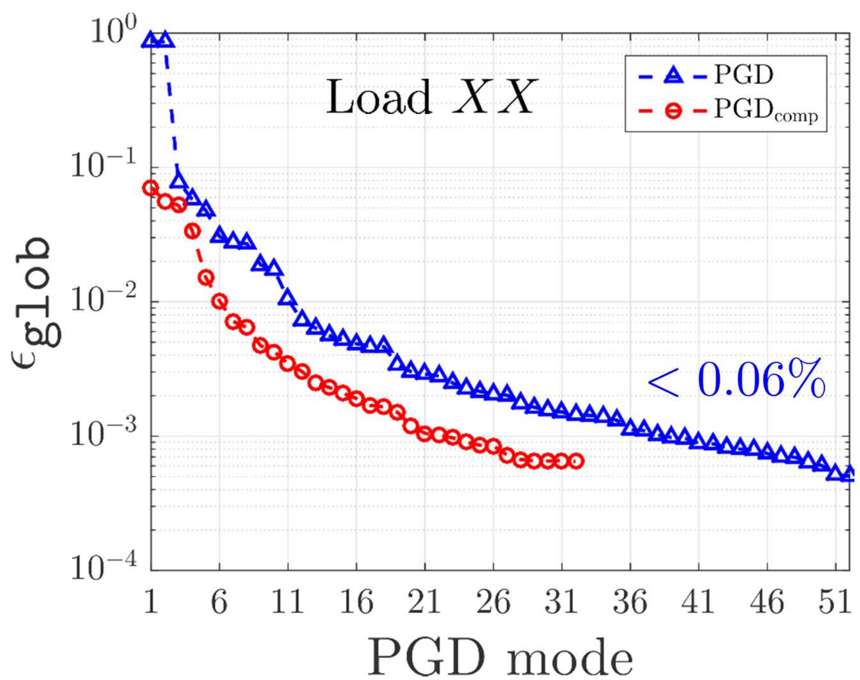

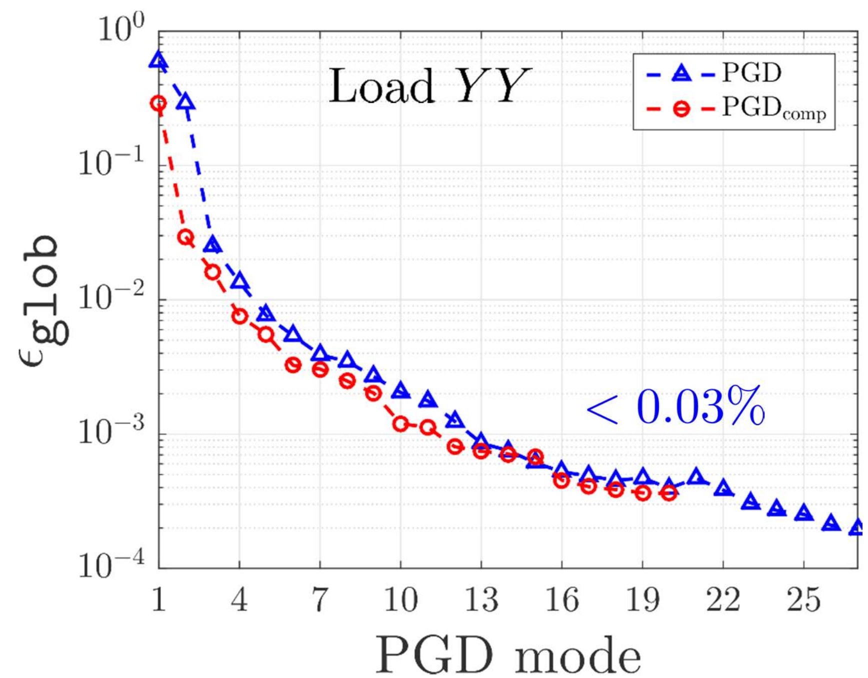

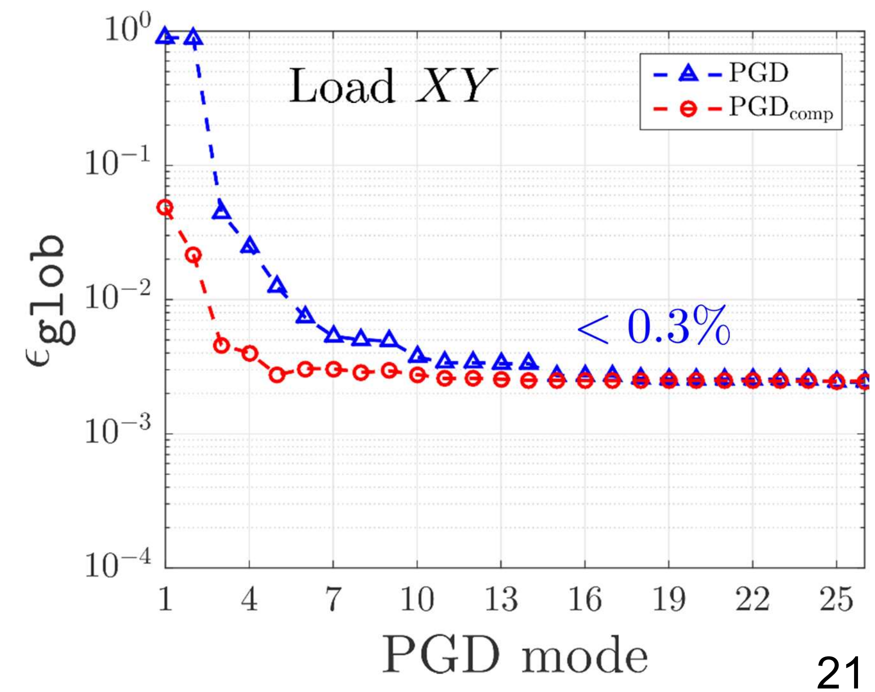

PGD local performance

- $\mathbf{U}_{\mathtt{PGD}}$ relative error at a particular set of values $(\boldsymbol{\mu} = \boldsymbol{\mu}_{\circ})$:

$$\epsilon_{\mathtt{local}}(\boldsymbol{\mu}_{\circ}) = \sqrt{\frac{(\mathbf{U}_{\mathtt{PGD}} - \mathbf{U})^{\mathsf{T}}\ \mathbf{M}\ (\mathbf{U}_{\mathtt{PGD}} - \mathbf{U})}{\mathbf{U}^{\mathsf{T}}\ \mathbf{M}\ \mathbf{U}}}.$$

- For each set $(\boldsymbol{\mu} = \boldsymbol{\mu}_{\circ})$, there is one error evolution curve.
- Local error decay is non-monotonic. Max. relative error: 2.5% for all loads.

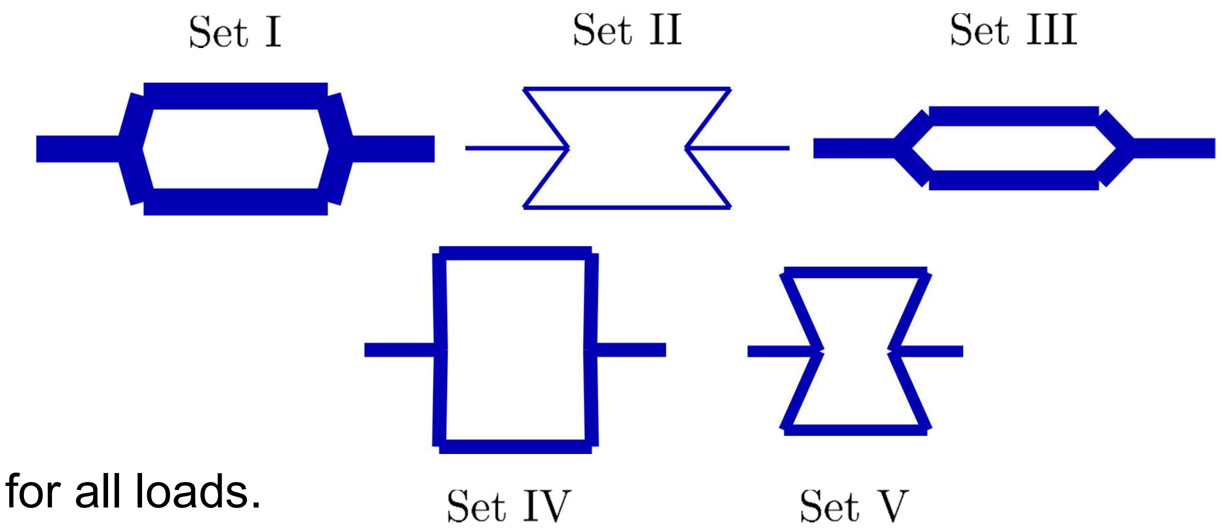

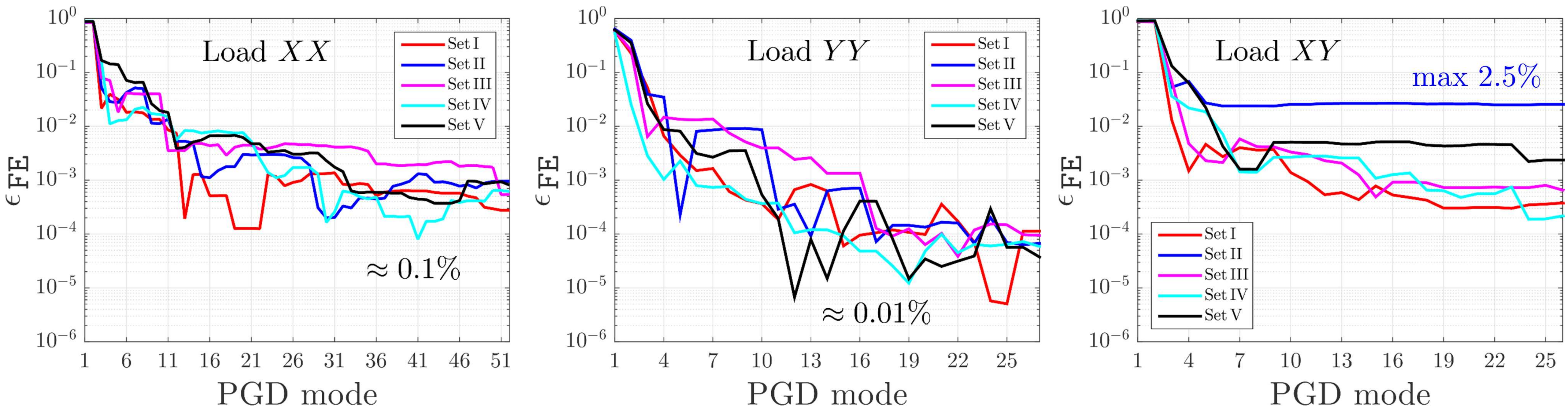

2D Effective Material Properties (Macro-scale)

- The material constitutive matrix $\mathbf{C}^{\,\mathtt{eff}}$ is recovered by upscaling the three unit-cell solutions (post-process).

$$\mathbf{C}^{\,\mathtt{eff}}(\boldsymbol{\mu}) = \begin{bmatrix} C_{11}^{\mathtt{eff}} & C_{12}^{\mathtt{eff}} & C_{13}^{\mathtt{eff}} \\ C_{21}^{\mathtt{eff}} & C_{22}^{\mathtt{eff}} & C_{23}^{\mathtt{eff}} \\ C_{31}^{\mathtt{eff}} & C_{32}^{\mathtt{eff}} & C_{33}^{\mathtt{eff}} \end{bmatrix}, \text{ Voigt notation in 2D.}$$

2D Orthotropic Poisson's Ratios ν_{12} and ν_{21}

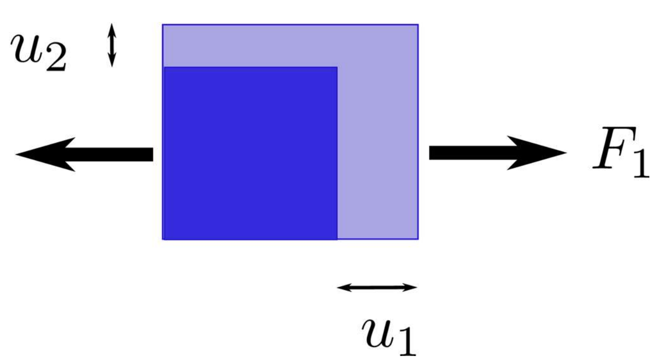

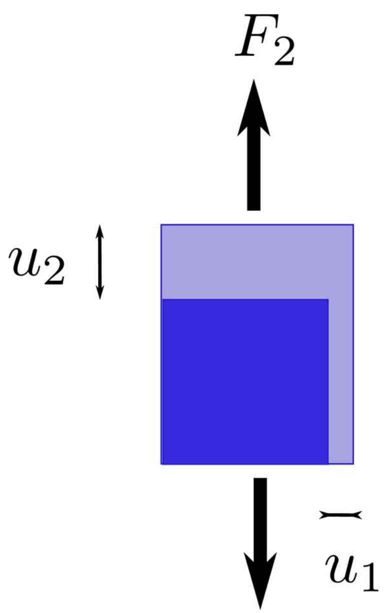

$$\nu_{12} = -\frac{u_2}{u_1}.$$

$$\nu_{21} = -\frac{u_1}{u_2}.$$

Honeycomb unit-cell + Homogenization

Effective Orthotropic Poisson's ratio $\nu_{12}^{\mathrm{eff}}(\boldsymbol{\mu})$

Upscaling: $$\nu_{12}^{\mathrm{eff}}(\boldsymbol{\mu}) = \frac{\mathrm{C}_{12}^{\mathrm{eff}}(\boldsymbol{\mu})}{\mathrm{C}_{22}^{\mathrm{eff}}(\boldsymbol{\mu})}.$$

4 snapshots in $(a \times \alpha)$:

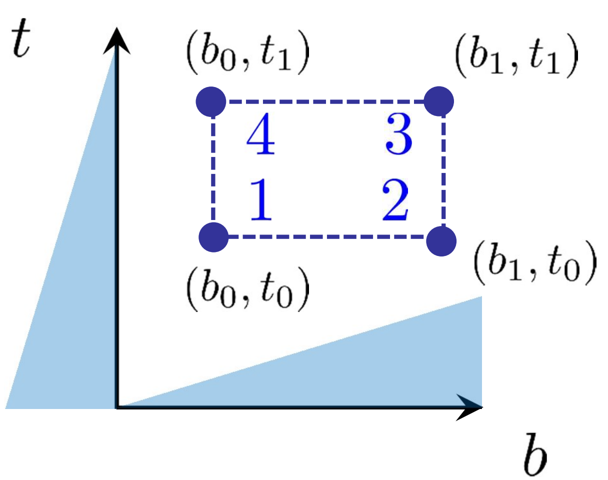

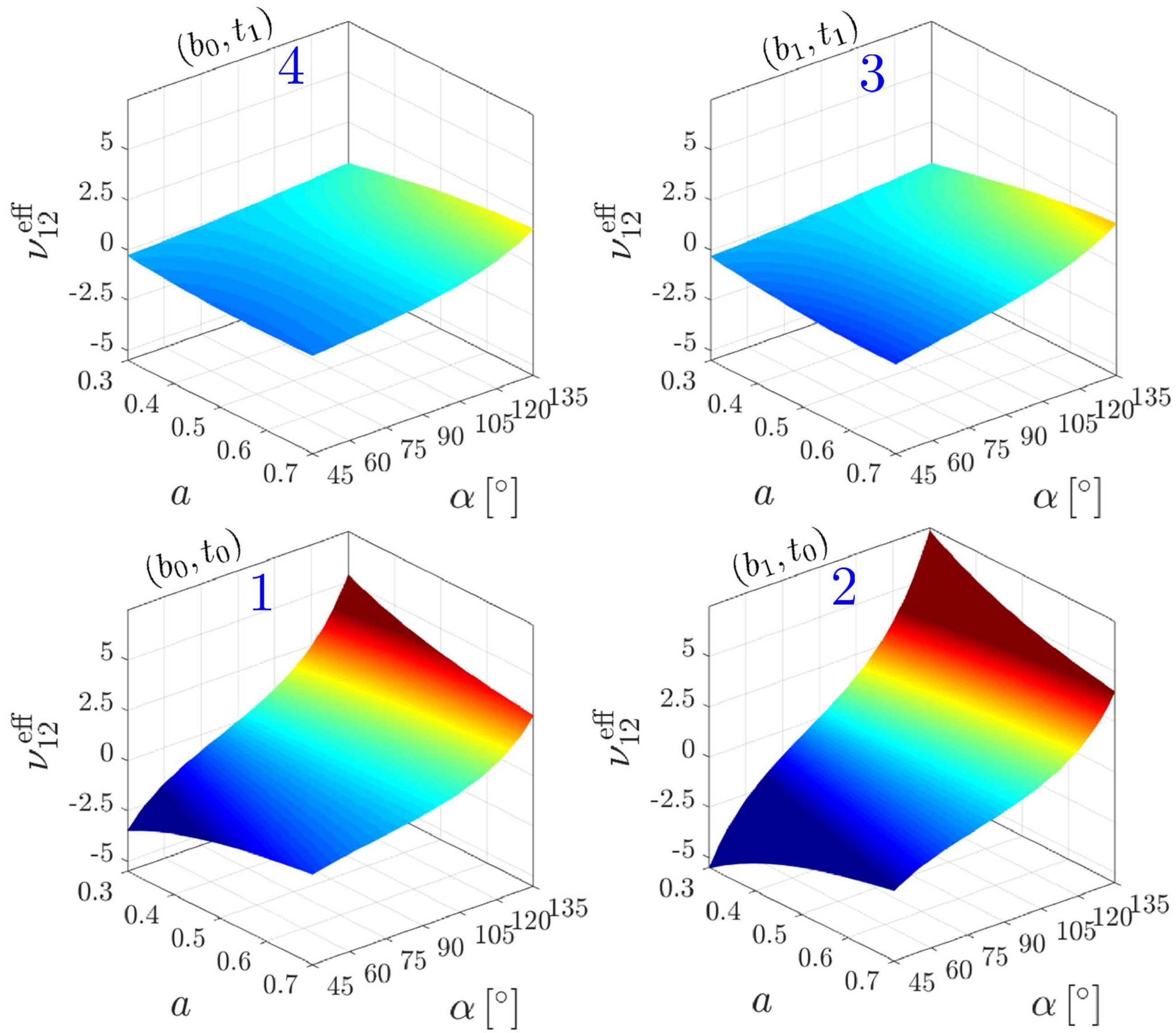

$\alpha < 90^\circ$:

Auxetic behavior.

Effective Orthotropic Poisson's ratio $\nu_{21}^{\mathrm{eff}}(\boldsymbol{\mu})$

Upscaling: $\nu_{21}^{\mathrm{eff}}(\boldsymbol{\mu}) = \dfrac{\mathrm{C}_{12}^{\mathrm{eff}}(\boldsymbol{\mu})}{\mathrm{C}_{11}^{\mathrm{eff}}(\boldsymbol{\mu})}$.

4 snapshots in $(a \times \alpha)$:

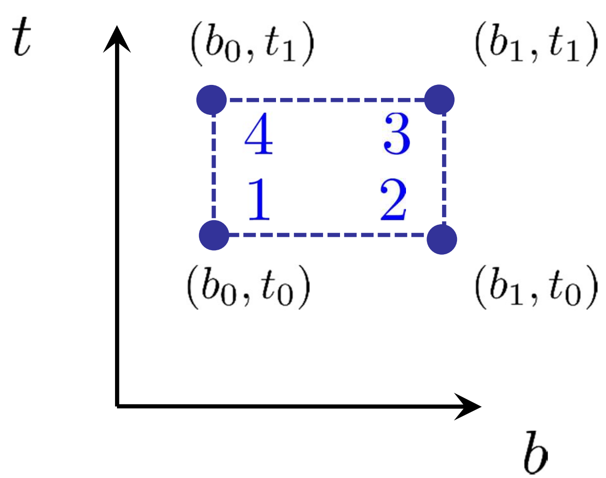

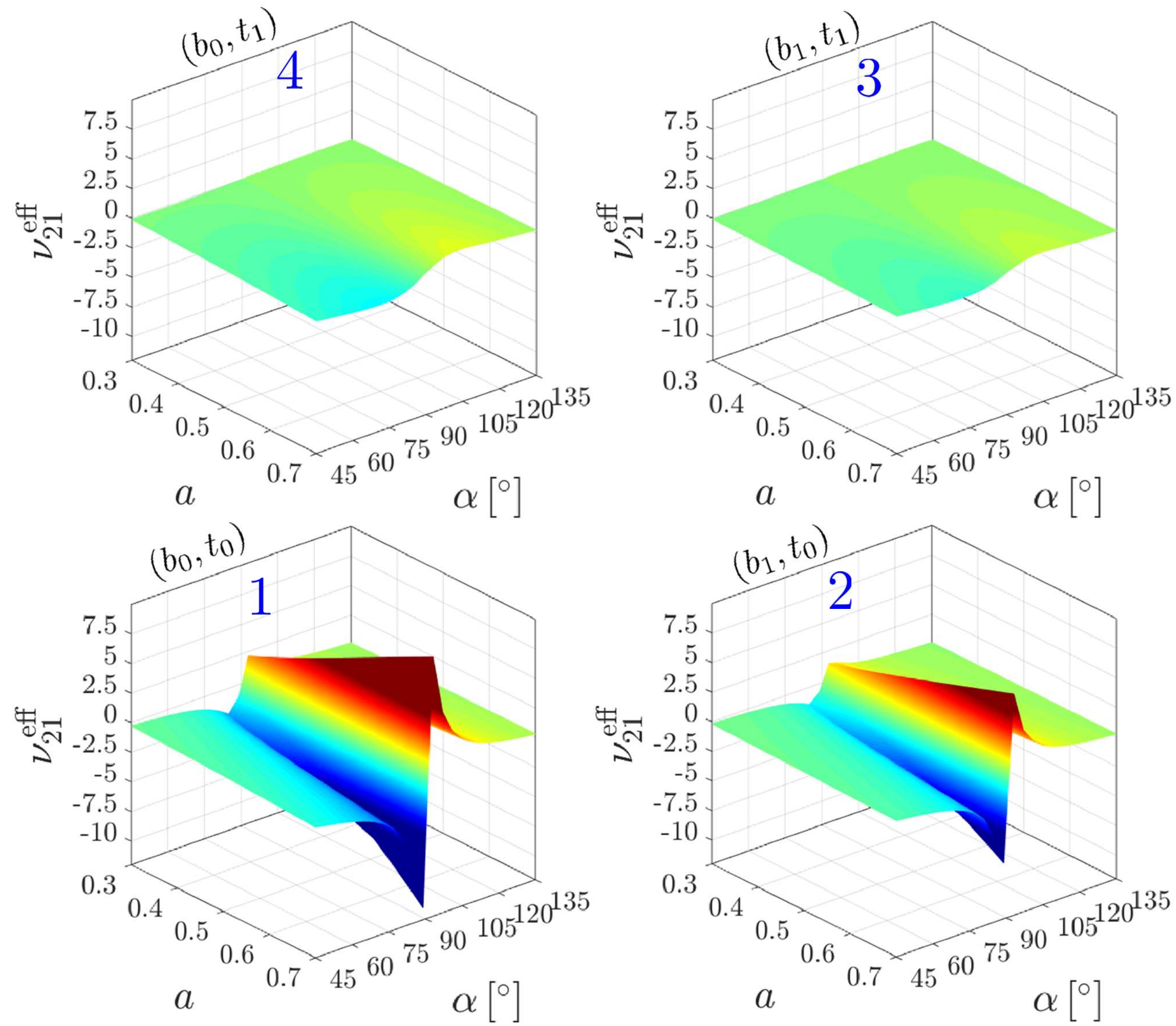

$\alpha < 90°$:

Auxetic behavior.

- Explicit parametric solutions:

3D lattice materials solved by Algebraic PGD

Unit-cell with Homogenization

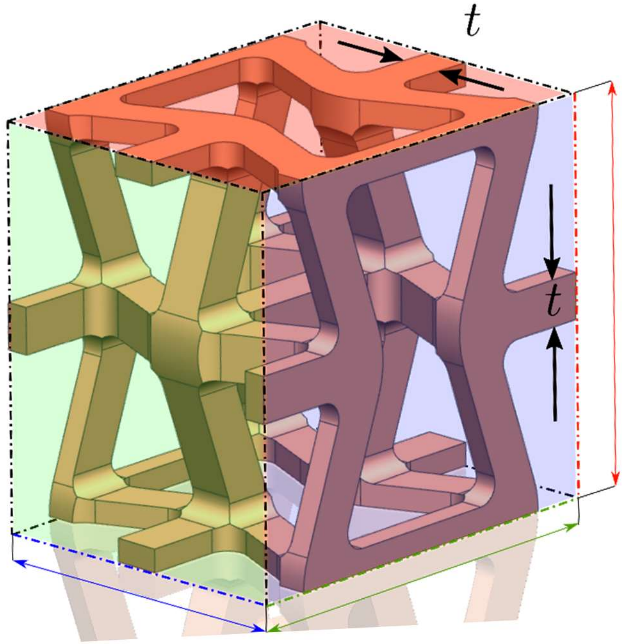

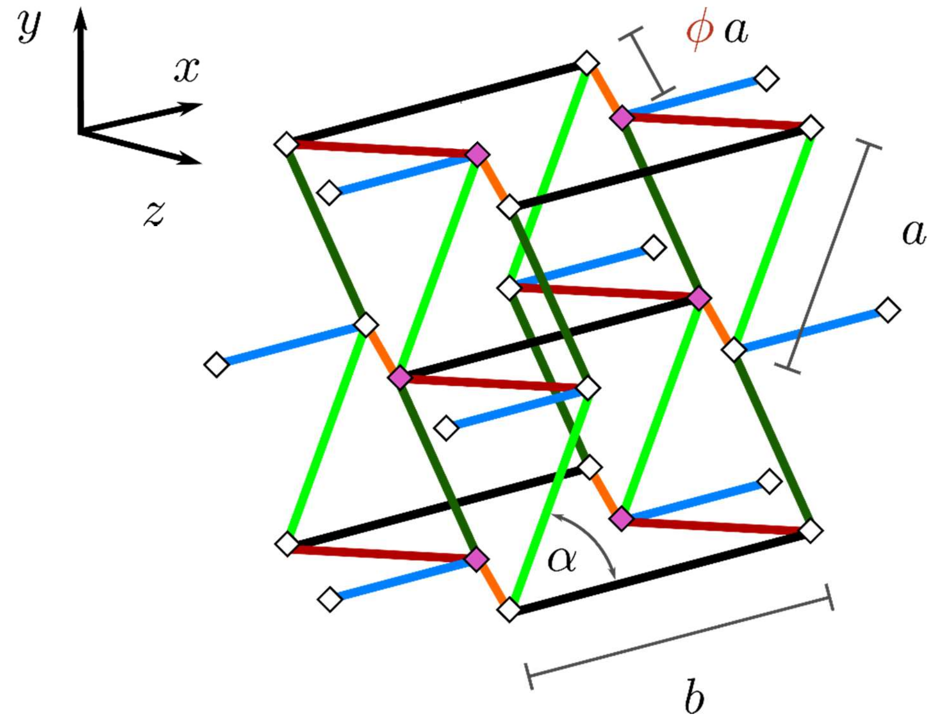

Geometry:

(xy planes): same parametrization of the hexagonal honeycomb
+
Scaffold aspect ratio in z

Parameters:

$$\boldsymbol{\mu} = [a\ b\ \alpha\ t\ \phi]$$

- Separable Input Data.
- Focus on the Poisson's ratios explicit parametric response.

3D Scaffold

Geometrical parametrization & Separable Input Data

- Main difference in geometrical parametrization *w.r.t.* 2D honeycomb is the equality constraint:

$$\cos(\alpha) = \phi \cos(\theta)\,.$$

- This ensures the structure connection at the points marked with:

- Then, the trigonometric functions required for our Input Data are:

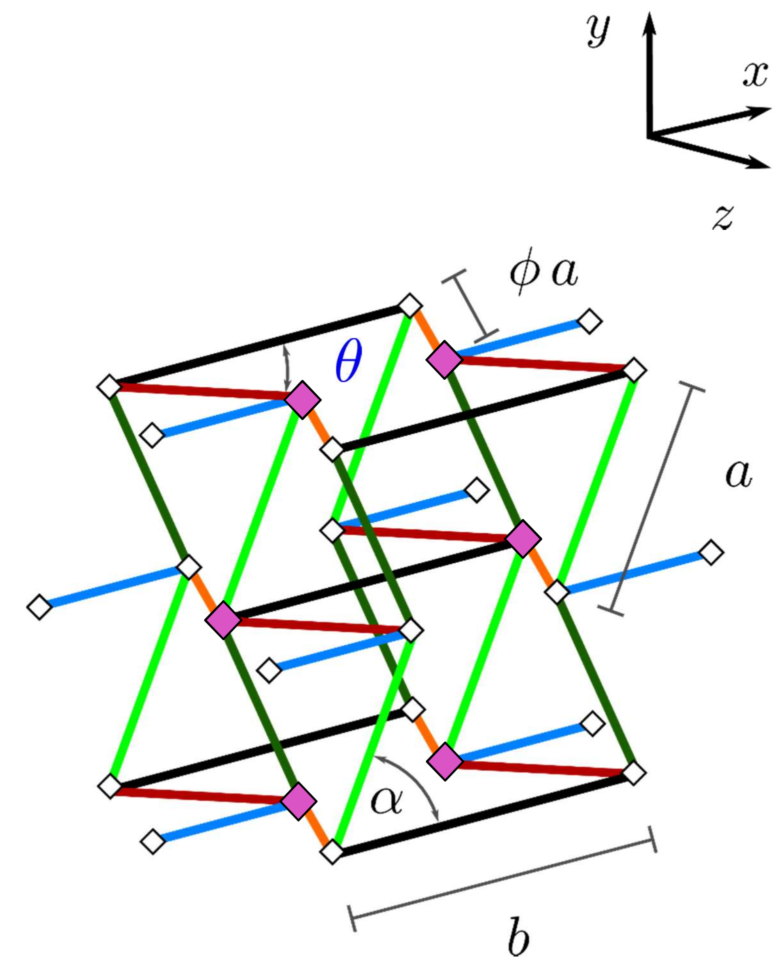

$$\begin{cases} \cos(\theta) := g(\alpha,\phi) = \dfrac{\cos(\alpha)}{\phi}\,, \\[2ex] \sin(\theta) := f(\alpha,\phi) = \sqrt{1-\dfrac{\cos^2(\alpha)}{\phi^2}} > 0 \;\; \forall(\alpha_0;\phi_0)\,. \end{cases}$$

Singular **V**alue **D**ecomposition: **SVD** $\longrightarrow$ $\mathbf{K}(\boldsymbol{\mu})$ $\longrightarrow$ Apgd

3D Orthotropic Material Properties

- The six unit-cell solutions are not shown, but the constitutive matrix $\mathbf{C}^{\,\mathtt{eff}}$ is recovered by upscaling.

$$\mathbf{C}^{\,\mathtt{eff}}(\boldsymbol{\mu}) = \begin{bmatrix} C^{\mathtt{eff}}_{11} & C^{\mathtt{eff}}_{12} & C^{\mathtt{eff}}_{13} & 0 & 0 & 0 \\ C^{\mathtt{eff}}_{21} & C^{\mathtt{eff}}_{22} & C^{\mathtt{eff}}_{23} & 0 & 0 & 0 \\ C^{\mathtt{eff}}_{31} & C^{\mathtt{eff}}_{32} & C^{\mathtt{eff}}_{33} & 0 & 0 & 0 \\ 0 & 0 & 0 & C^{\mathtt{eff}}_{44} & 0 & 0 \\ 0 & 0 & 0 & 0 & C^{\mathtt{eff}}_{55} & 0 \\ 0 & 0 & 0 & 0 & 0 & C^{\mathtt{eff}}_{66} \end{bmatrix}.$$

3D Orthotropic Poisson's Ratios

- Six orthotropic Poisson's ratios result at the macro-scale. Results will focus on $\nu^{\mathrm{eff}}_{23}(\boldsymbol{\mu})$ to analyze the PGD solver accuracy.

Effective Orthotropic Poisson's ratio $\nu_{23}^{\mathrm{eff}}(\boldsymbol{\mu})$.

<u>Upscaling:</u> $\nu_{23} = \dfrac{C_{12}\,C_{13} - C_{11}\,C_{23}}{(C_{13})^2 - C_{11}\,C_{33}}.$

<u>4 snapshots</u> in $(\phi \times \alpha)$:

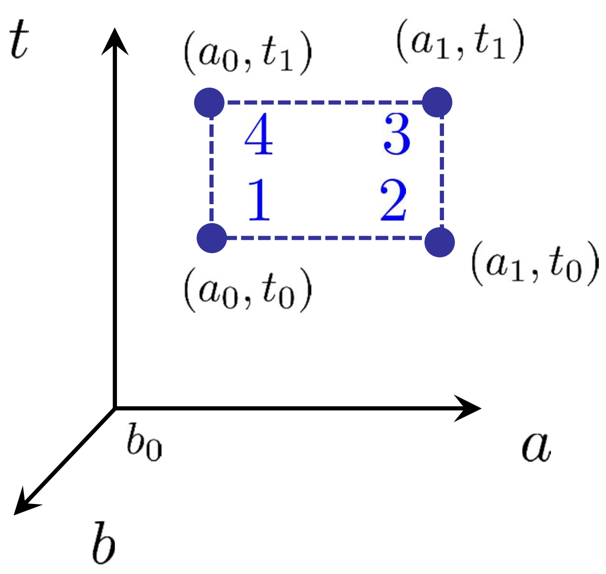

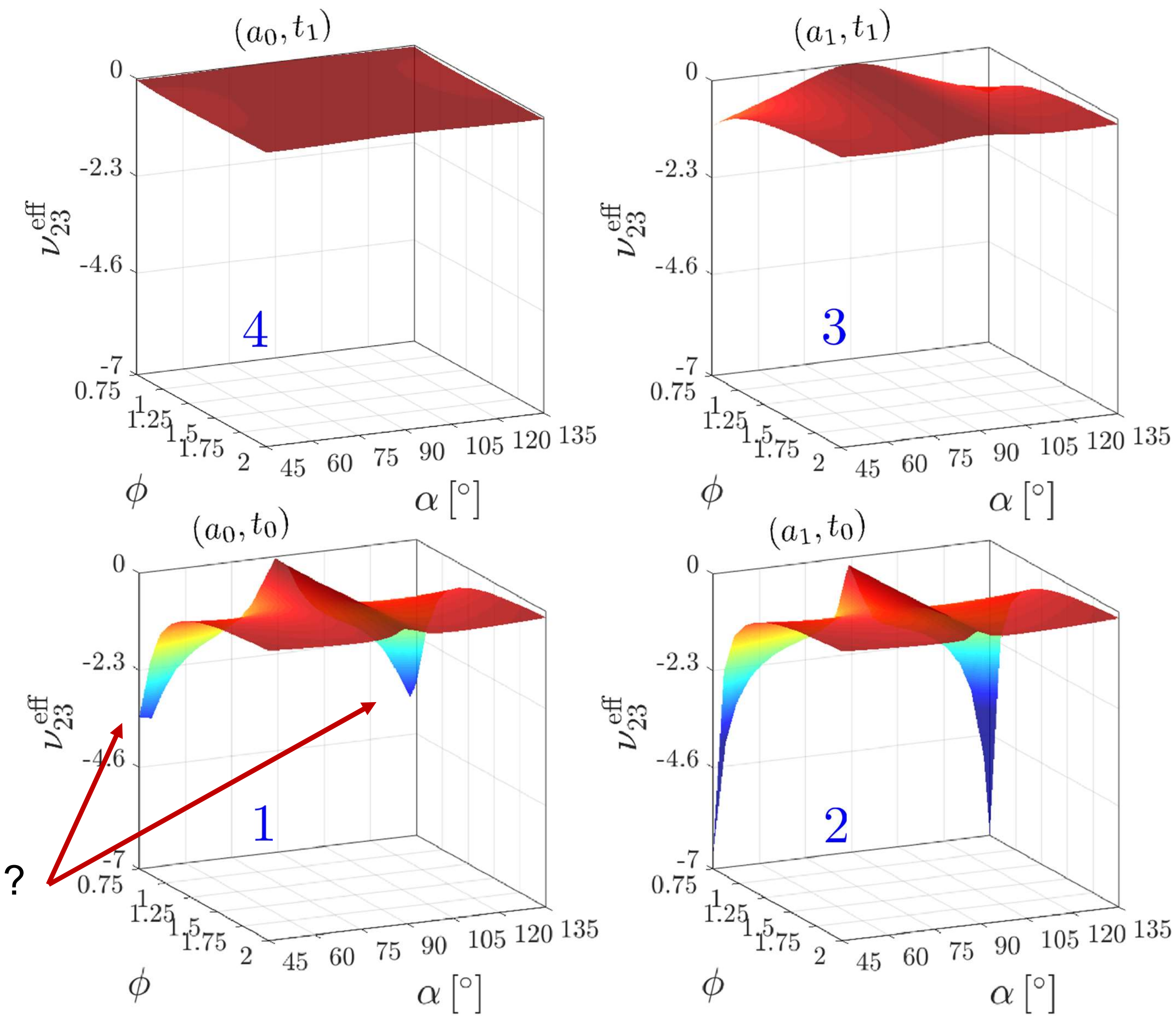

Are these peaks well captured?

Auxetic for all parameters ranges

Poisson's ratio $\nu_{23}^{\text{eff}}(\boldsymbol{\mu})$ accuracy

- Relative error of the PGD response below, against finite elements:

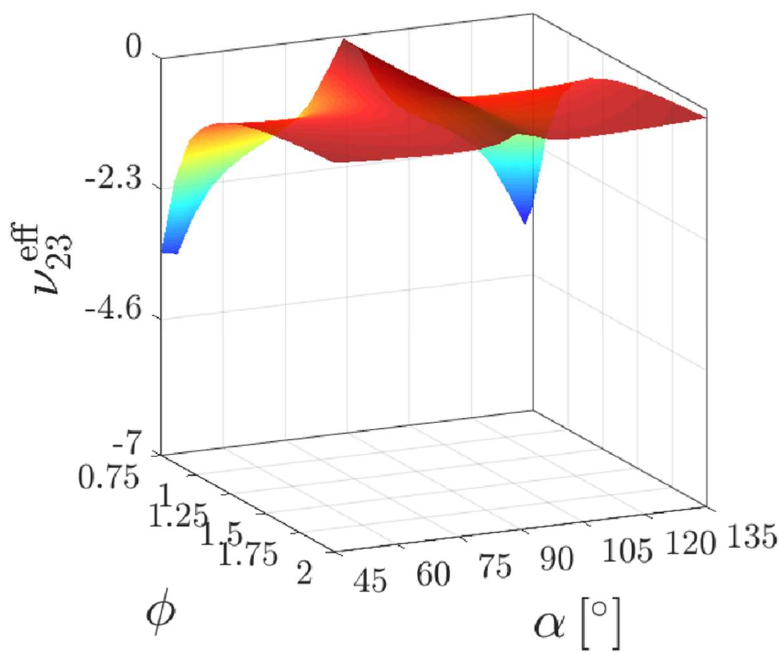

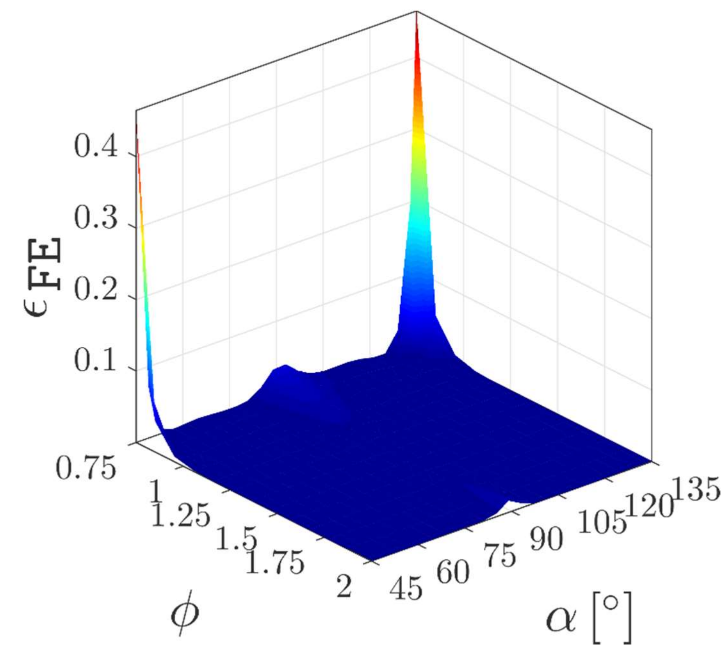

- At peak values of $\nu_{23}^{\text{eff}}(\boldsymbol{\mu})$, the relative error raises above 40%.
- Particularity: PGD unit-cell solutions relative errors are below 3%, but these are amplified by the upscaling:

$$\nu_{23}^{\text{eff}}(\boldsymbol{\mu}) = \frac{C_{12}\,C_{13} - C_{11}\,C_{23}}{(C_{13})^2 - C_{11}\,C_{33}}.$$

Material Structure

5x5x5 unit-cells pattern:

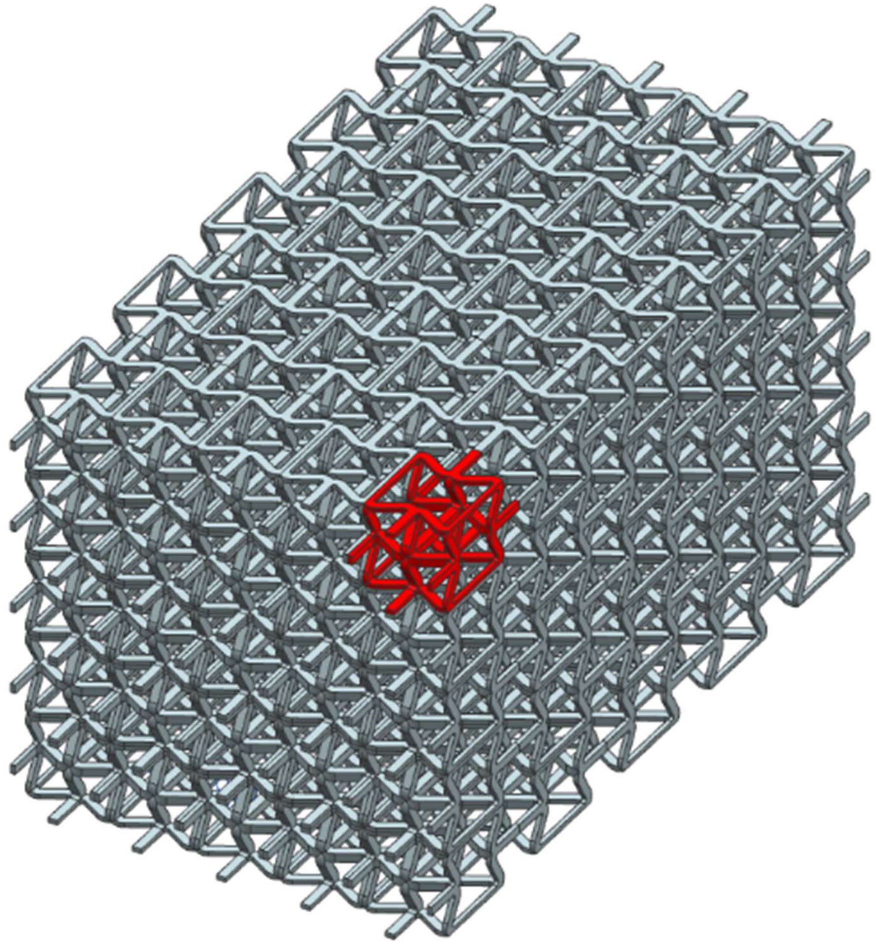

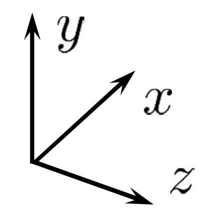

- The material structure is subjected to uni-axial loads.
- I will use this material structure to asses the PGD accuracy where high errors of $\nu_{23}^{\text{eff}}(\boldsymbol{\mu})$ were found using homogenization.

PGD local performance

- Deformed structures between FE and PGD for uni-axial load *Y*. Set of parameters: $\boldsymbol{\mu}_0$

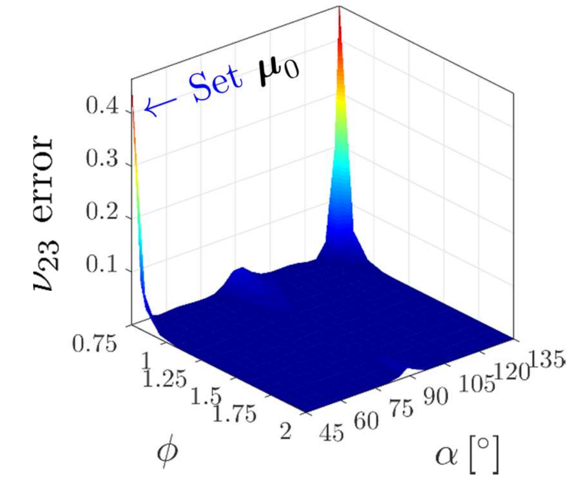

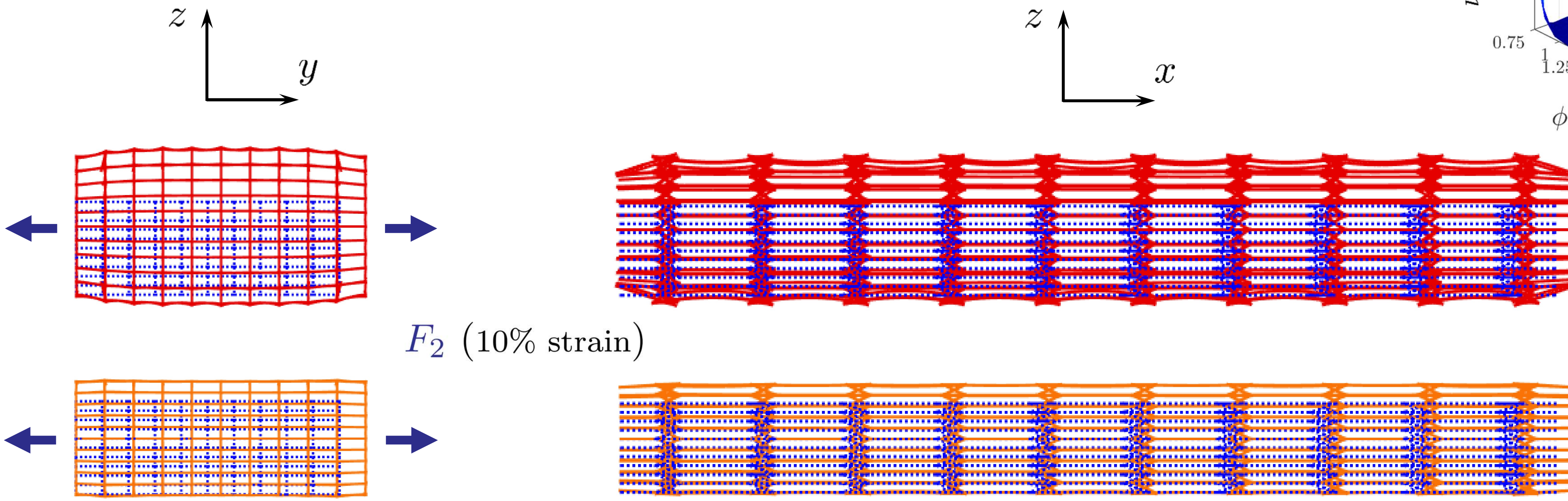

- Displacements in "z" direction are notably "locked" (PGD *w.r.t.* FE), in correspondence to ν_{23}^{eff} error.
- Immediate actions: local refinement or higher order approximating functions for the parameters. PGD advantage: refining affects only 1D problems separately, the costs do not propagate globally.

- PGD least-squares approximation for nonlinear lattice structures.

Motivations in Lattice Materials

- Buckling, a meaningful effect.

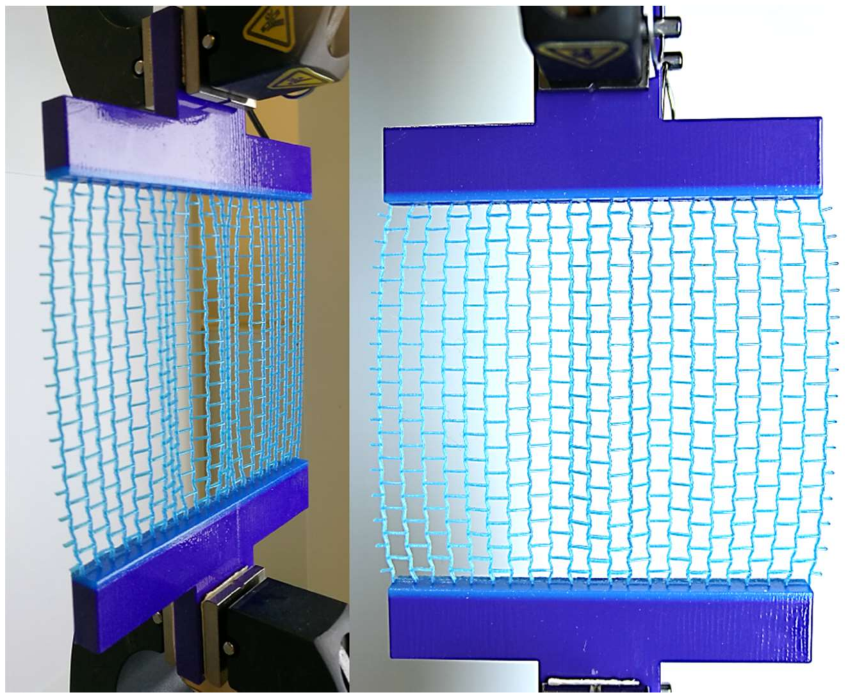

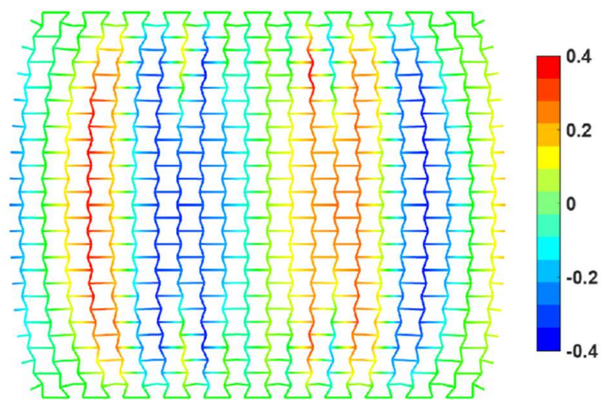

- Extreme Poisson's ratios: full range of applicability.

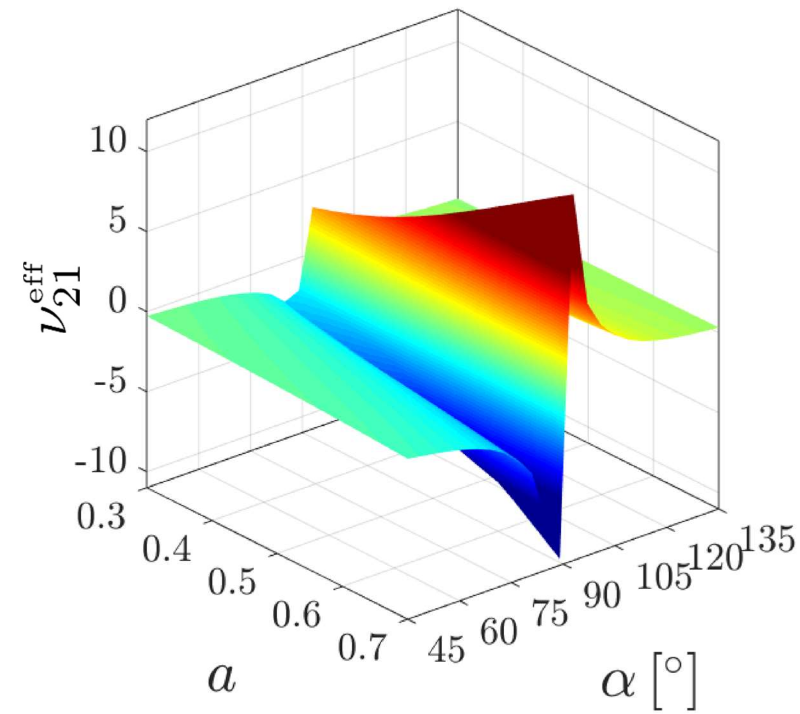

A posteriori PGD for geometrical nonlinearities

Stent Load Cases (Radial – Axial)

$$\boldsymbol{\mu} = [a\ \cancel{b}\ \alpha\ \cancel{t}].$$

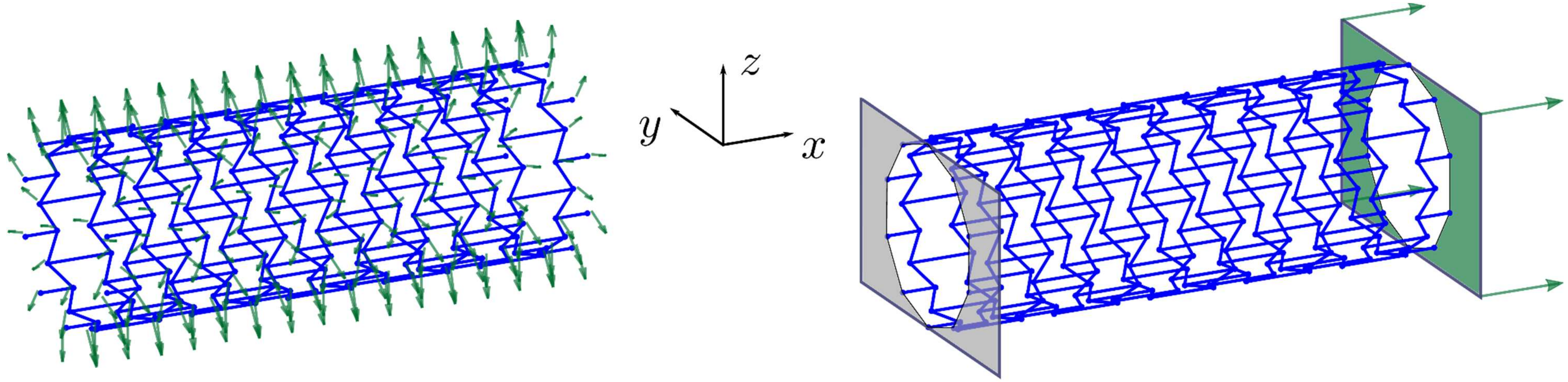

Multidimensional sampling – Parametric Stent

- Two geometrical parameters, b and t are fixed to reduce the amount of combinations.
- Finite element solutions are run at prescribed values of the parameters.

Beam model

- Large displacements and small strains, finite element software: ADINA.
- Nonlinear strain-displacements relation + linear elastic strain-stress relation.
- Incremental load steps: loading parameter $\lambda \quad \Rightarrow \quad \boldsymbol{\mu}_{\mathtt{nl}} = [a\ \alpha\ \lambda].$

A posteriori PGD for geometrical nonlinearities

Method

- Equilibrium configurations (displacements + rotations) are stored in a multidimensional tensor.
- Size of this tensor: $(n_a \times n_\alpha \times n_\lambda)$, $n_a = 50$, $n_\alpha = 91$ $n_\lambda = 10$.
- PGD least-squares provides a separated approximation of the multidimensional tensor.
- Same PGD compression algorithm, different input data (multidimensional instead of a separated tensor).

Results

- Explicit parametric solutions (with loading magnitude as an extra parameter).
- Very good accuracy is achieved without an excessive amount of modes.
- General concept: no gain in computational cost, significant reductions in terms of storage.

PGD Least-Squares approximation – Modal Amplitudes

- Two load cases (Radial – Axial).

Stop Greedy if: $$\frac{\beta^n}{\max_{m=1,\ldots,n}(\beta^m)} < 10^{-3}.$$

- Same Greedy stopping criteria for the two loads.
- Total number of modes for the Axial load is significantly higher (response prompt to buckling).

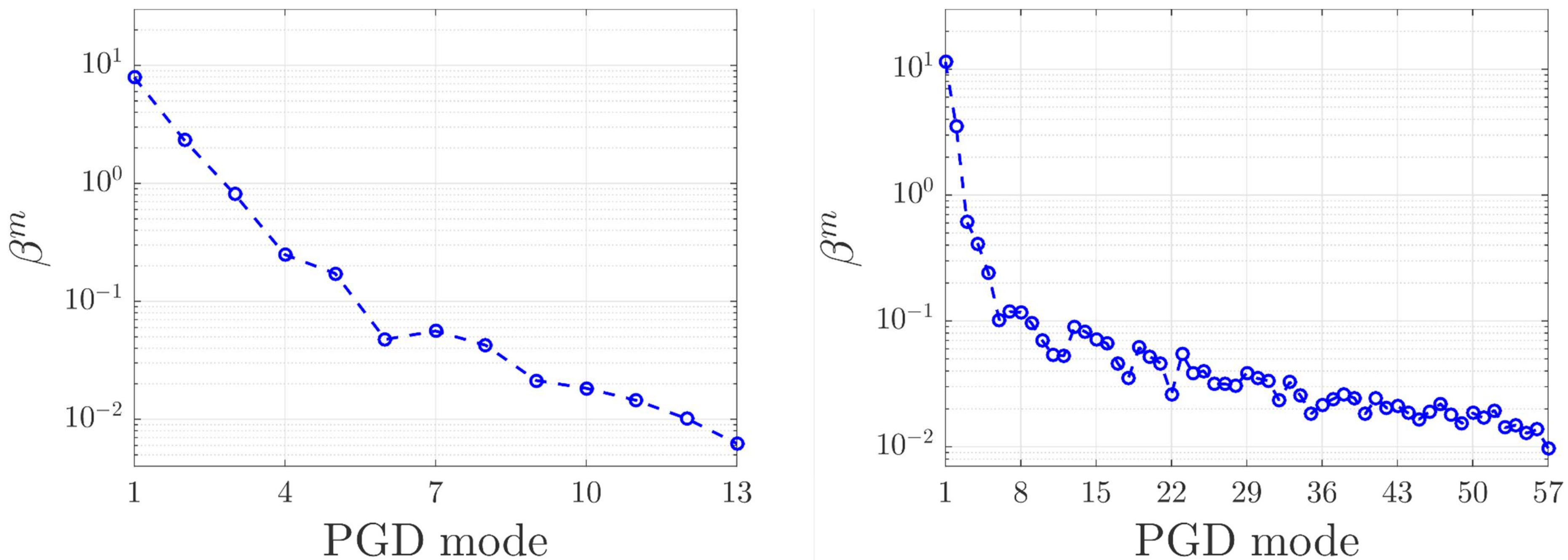

(a) Radial load (b) Axial load

Radial Load – Linear vs. Nonlinear response $\nu_{\texttt{rad-ax}}(\boldsymbol{\mu})$ vs. $\nu_{\texttt{rad-ax}}(\boldsymbol{\mu}_{\texttt{nl}})$

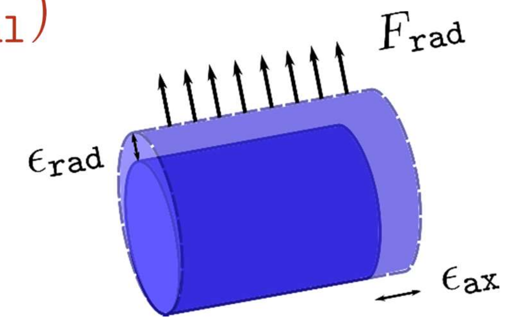

- Plot in $(a \times \alpha)$, 4 different snapshots (Linear, NL: $\lambda = 1$, NL: $\lambda = 5$, and NL: $\lambda = 10$).
- Novelty: mechanical property depending on loading parameter λ.
- For a small loading magnitude, nonlinear and linear response match.
- $\nu_{\texttt{rad-ax}}$ extreme values change in magnitude and parametric location by the loading parameter λ.

$$\nu_{\texttt{rad-ax}} = -\frac{\epsilon_{\texttt{ax}}}{\epsilon_{\texttt{rad}}}.$$

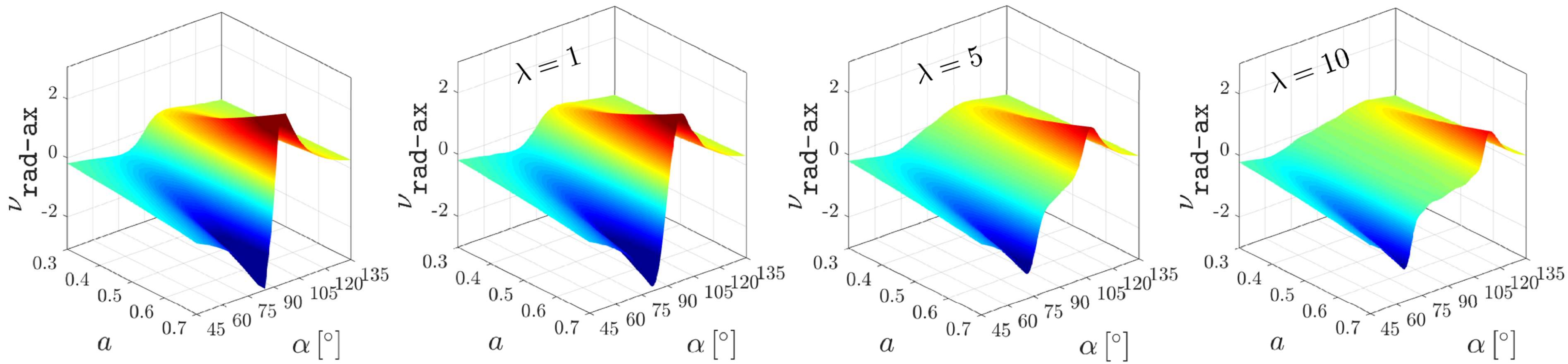

(a) Linear — Algebraic PGD solver

(b) Loaded strain 1% — A posteriori PGD

(c) Loaded strain 5% — A posteriori PGD

(d) Loaded strain 10% — A posteriori PGD

Axial Load – Linear vs. Nonlinear response $\nu_{\texttt{ax-rad}}(\boldsymbol{\mu})$ vs. $\nu_{\texttt{ax-rad}}(\boldsymbol{\mu}_{\texttt{nl}})$

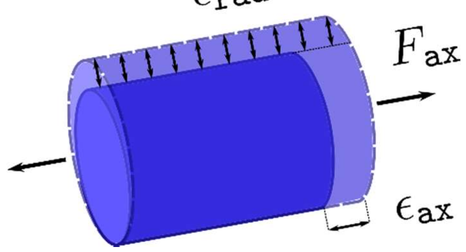

- Plot in $(a \times \alpha)$, 4 different snapshots (Linear, NL: $\lambda = 1$, NL: $\lambda = 5$, and NL: $\lambda = 10$).
- Novelty: mechanical property shows the presence of *buckling* instabilities.
- Small loading magnitude: nonlinear and linear response match (despite some noise).
- Higher auxetic behavior and higher $\lambda \Rightarrow$ more buckling.
- The buckled shape reduces the stent radius locally → lower $\nu_{\texttt{ax-rad}}$.

$$\nu_{\texttt{ax-rad}} = -\frac{\bar{\epsilon}_{\texttt{rad}}}{\epsilon_{\texttt{ax}}}.$$

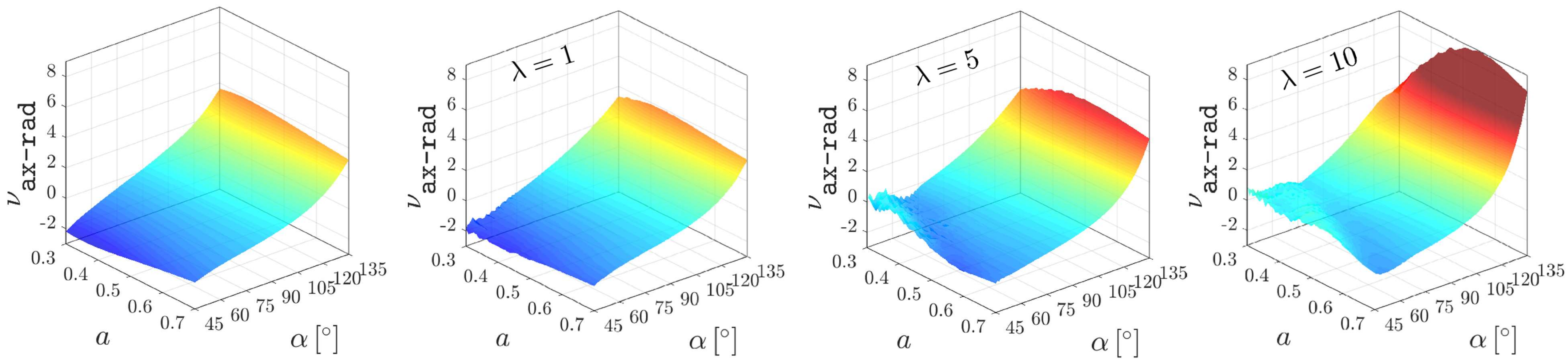

(a) Linear — Algebraic PGD solver

(b) Loaded strain 1% — A posteriori PGD

(c) Loaded strain 5% — A posteriori PGD

(d) Loaded strain 10% — A posteriori PGD

Interactive parametric buckling analysis

- A linear (in Red) vs. nonlinear (in Green) PGD solutions of the stent are post-processed interactively in a user-friendly web application (HTML based).

- Concluding remarks & Future works.

Concluding Remarks

- This thesis contributed to the algebraic PGD solver development. In addition, it proves its value as a powerful tool to input different lattice material structures and output explicit parametric solutions.
- The separation of input data for algebraic PGD in lattice structures is carried out using an integrated approach of finite element procedures with the parametric dimension.
- A user-friendly web app has been develop to display interactively and in real time, parametric solutions of lattice materials and its mechanical properties. This contributes to broaden the applicability of PGD in non-academic environments.
- The least-squares PGD approximation has been introduced as an approach that "*learns from nonlinear finite elements data*". In lattice materials, mechanical properties and buckling effects are successfully obtained as explicit functions of geometrical parameters and a loading magnitude.

Future Works

- Regarding material design with tailored properties, this thesis presents a groundwork on top of which the PGD vademecum could be further exploited for multi-objective and constrained optimizations.
- Lack of accuracy of the algebraic PGD at some of the Poisson's ratio extreme values should be tackled using local refinement or higher order approximating functions in the parametric space.
- Explicit parametric solutions constructed a priori for geometrically nonlinear lattices deserve future research efforts. The feasibility of using algebraic PGD to this end is subjected to the affine decomposition of the residual equation.
- A more precise criterion to stop the greedy computation of modes could be based on an error estimation of the residual or some quantity of interest.
- In structural analysis, buckling is assed through the solution of an eigenvalue problem. Adopting this framework to a parametric setting, and efficiently solve the eigenvalue problem would result in a highly valuable tool for lattice materials and structures.

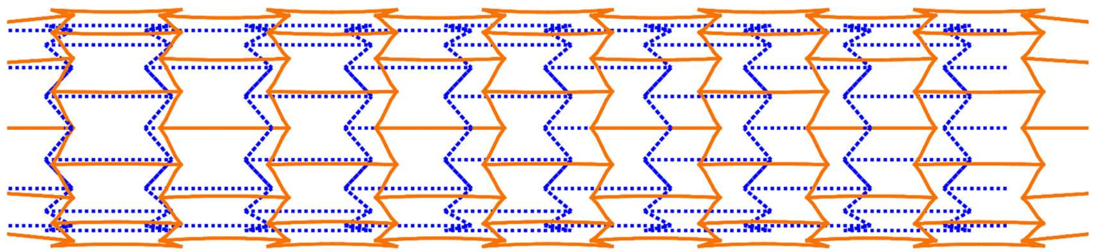

And thank you all !!!